

# Temporal variation of $^{129}\text{I}$ and $^{127}\text{I}$ in aerosols from Xi'an, China: influence of East Asian monsoon and heavy haze events

Luyuan Zhang <sup>1,2,5\*</sup>, Xiaolin Hou <sup>1,2,3,5</sup>, Sheng Xu <sup>4</sup>, Tian Feng <sup>1</sup>, Peng Cheng <sup>1</sup>, Yunchong Fu <sup>1</sup>, Ning Chen <sup>1</sup>

**Formatted:** Font: (Default) Times New Roman, (Asian) Times New Roman

5 <sup>1</sup>State Key Laboratory of Loess and Quaternary Geology, Shaanxi Key Laboratory of Accelerator Mass Spectrometry Technology and Application, Xi'an AMS Center, Institute of Earth Environment CAS, Xi'an 710061, China

<sup>2</sup>Center for Excellence in Quaternary Science and Global Change, Chinese Academy of Sciences, Xian 710061, China

<sup>3</sup>Center for Nuclear Technologies, Technical University of Denmark, Risø Campus, Roskilde 4000, Denmark

<sup>4</sup>Institute of Surface-Earth System Science, Tianjin University, Tianjin 300072, China

10 <sup>5</sup>Open Studio for Oceanic-Continental Climate and Environment Changes, Pilot National Laboratory for Marine Science and Technology (Qingdao), Qingdao 266061, China

Correspondence to: Luyuan Zhang (zhangluyuan.118@163.com)

**Formatted:** Superscript

**Formatted:** Font: Times New Roman

**Formatted:** (Asian) Chinese (China), (Other) English (US)

**Abstract.** Aerosol iodine isotopes are pivotal links in atmospheric circulation of iodine in both atmospheric and nuclear sciences, while their sources, temporal change and transport mechanism are still not well understood. This work presents the 15 day-resolution temporal variation of iodine-129 ( $^{129}\text{I}$ ) and iodine-127 ( $^{127}\text{I}$ ) in aerosols from Xi'an, northwest China during 2017/2018. Both iodine isotopes have significant fluctuations with time, showing highest levels in winter, approximately two to three times higher than in other seasons, but the correlation between  $^{129}\text{I}$  and  $^{127}\text{I}$  reflects they have different sources. Aerosol  $^{127}\text{I}$  is found to be noticeably positively correlated with air quality index and five air pollutants. Enhanced fossil fuel combustion and inverse weather conditions can explain the increased concentrations and peaks of  $^{127}\text{I}$  in winter. The change of  $^{129}\text{I}$  confirms 20 that source and level of  $^{129}\text{I}$  in the monsoonal region were alternatively dominated by the  $^{129}\text{I}$ -enriched East Asian winter monsoon and the  $^{129}\text{I}$ -poor East Asian summer monsoon. The mean  $^{129}\text{I}/^{127}\text{I}$  atomic ratio of  $(92.7 \pm 124) \times 10^{-10}$  provides an atmospheric background level for the purpose of nuclear environmental safety monitoring. This study suggests that locally discharged stable  $^{127}\text{I}$  and externally input  $^{129}\text{I}$  are likely involved into fine particles formation in urban air, shedding insights 25 into long-range transport of air pollutants and iodine's role in particulate formation in urban atmosphere.

**Formatted:** Not Highlight

**Deleted:**  $101 \pm 124$

**Formatted:** (Asian) Chinese (China), (Other) English (US)

## 25 1 Introduction

Iodine is one of active halogen elements, and involved into plenty of atmospheric chemical reactions (i.e. ozone depletion and new particles formation from condensable iodine-containing vapours), drawing increasing attention in not only atmospheric science, but also environmental fields in recent years (Saiz-Lopez et al., 2012). A number of studies on atmospheric iodine just focus on the processes and mechanisms in marine boundary layer since over 99.8% of iodine derives from ocean 30 (McFiggans et al., 2000). Other sources of iodine in air comprise volatile iodine and resuspended particles from soil, as well

as combustion of fossil fuel (Fuge and Johnson, 1986). Whitehead et al. (1984) estimated annual release of iodine from fossil fuel combustion is about 400 tons, accounting for only 0.1% of total iodine in air. Whereas, anthropogenic iodine in Chinese megacities is believed to be significantly underestimated due to coal combustion (Wu et al., 2014). ~~A few studies have shown~~

35 high iodine concentrations in air and particles in China (Gao et al., 2010; Xu et al., 2010). Although marine atmospheric iodine has been proven to form fine particles, little is known about terrestrial atmospheric iodine, particularly in urban sites with severe air pollution.

Along with atmospheric circulation of stable  $^{127}\text{I}$ , long-lived radioactive  $^{129}\text{I}$  with half-life of 15.7 million years is also of importance in global transport since it is a major fission product with ~~a~~ yield of 0.7% in nuclear industry. China is in transition 40 phase of energy structure to solve ~~environmental pollution issues~~, and has put great emphasis on developing nuclear power (World Nuclear Association, 2017). Nuclear waste reprocessing is ~~also~~ in the process of construction in China, which may be a key source of  $^{129}\text{I}$  in the future. Investigation on level, sources, temporal changes are extremely necessary for nuclear environmental safety assessment and nuclear emergency preparedness. Environmental  $^{129}\text{I}/^{127}\text{I}$  atomic ratios have been increased from natural  $^{129}\text{I}$  level of  $10^{-12}$  to anthropogenic level beyond  $10^{-10}$  in modern environment due to the atmospheric

45 nuclear weapon testing, nuclear accidents, nuclear fuel reprocessing process, ~~etc~~ (Snyder et al., 2010). More than 95% of the environmental  $^{129}\text{I}$  was discharged by the two European nuclear fuel reprocessing plants (NFRPs), Sellafield in United Kingdom and La Hague in France to the seas and air in liquid and gaseous forms, ~~respectively~~. As a consequence of  $^{129}\text{I}$  releases from NFRPs, nuclear accidents and nuclear weapon testing sites, the ~~global~~ distribution of  $^{129}\text{I}$  is rather uneven (Snyder et al., 2010). Atmospheric  $^{129}\text{I}$  investigations have been conducted in Europe, Japan, USA and Canada, but aerosol  $^{129}\text{I}$  studies

50 are still rare, and no aerosol  $^{129}\text{I}$  data is available in China at present (Hasegawa et al., 2017; Hou et al., 2009; Jabbar et al., 2013; Moran et al., 1999; Toyama et al., 2013; Xu et al., 2013). ~~Furthermore~~, ~~those~~ previous studies present time series of  $^{129}\text{I}$  in aerosols in monthly resolution for the purpose of nuclear environmental monitoring. ~~Such a~~ low time-resolution is not sufficient to understand the sources, transport and temporal variation pattern and its influencing factor of  $^{129}\text{I}$ .

Here, we present a day-resolution temporal variation of  $^{129}\text{I}$  and  $^{127}\text{I}$  in aerosols during 2017/2018 from a typical monsoonal 55 zone, Xi'an city in the Guanzhong Basin of ~~northwest~~ China, to make attempts to investigate the level, sources and temporal change characteristics of  $^{127}\text{I}$  and  $^{129}\text{I}$ . ~~This study will help~~ to establish a background value of  $^{129}\text{I}/^{127}\text{I}$  ratio serving the nuclear environmental safety monitoring. ~~The possible~~ influencing factors on temporal variation of iodine isotopes are also explored, including meteorological parameters, East Asian monsoon (EAM) and heavy haze events. ▲

**Deleted:** (Whitehead, 1984)

**Deleted:** Few

**Deleted:** found

**Deleted:** the

**Deleted:** Furthermore, n

**Deleted:** these point sources of  $^{129}\text{I}$ ,

**Field Code Changed**

**Deleted:** ; Xu et al., 2015

**Deleted:** T

**Deleted:** e

**Deleted:** the

**Deleted:** ,

**Deleted:** while the

**Deleted:** northwest

**Deleted:** of

**Deleted:** ,

**Deleted:** , as well as to make clear

**Deleted:** key

**Formatted:** English (US)

**Formatted:** (Asian) Chinese (China), (Other) English (US)

**Deleted:** by

**Deleted:** the

**Deleted:** re

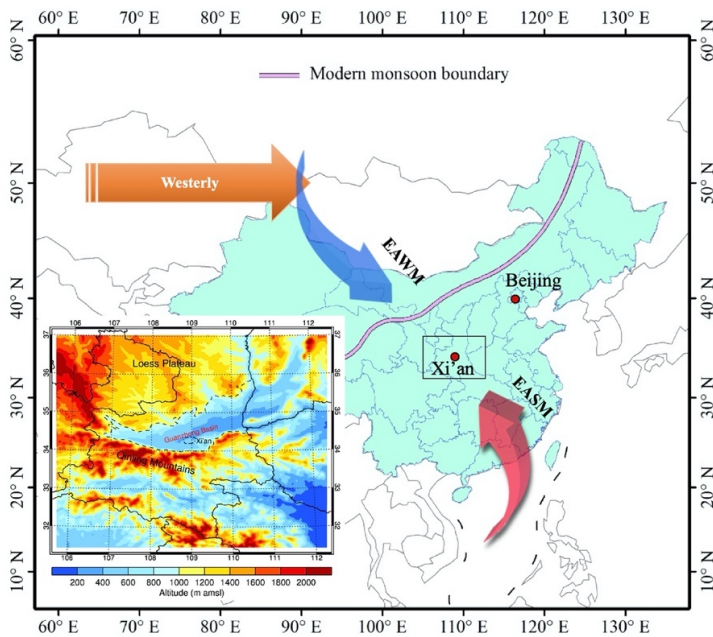
**Deleted:** in Xi'an, China

**Deleted:** the

**Deleted:**

**Deleted:** L

90 ~~Sixty-eight aerosol samples were selected for measurement of iodine isotopes using the pyrolysis combined with AgI-AgCl coprecipitation for separation. The sample collection and preparation procedure are described in detail in the supplementary information (SI-1), as previously reported (Zhang et al., 2018b). Accelerator mass spectrometry (AMS, 3MV, HVEE, the Netherland) and inductively coupled plasma mass spectrometry (ICP-MS, Agilent 8800, USA) were applied for determination of  $^{129}\text{I}/^{127}\text{I}$  ratios and  $^{127}\text{I}$  concentrations, respectively.  $^{129}\text{I}/^{127}\text{I}$  atomic ratio of iodine carrier is less than  $2 \times 10^{-13}$ , and the analytical precision are within 5% for all the aerosol samples.~~



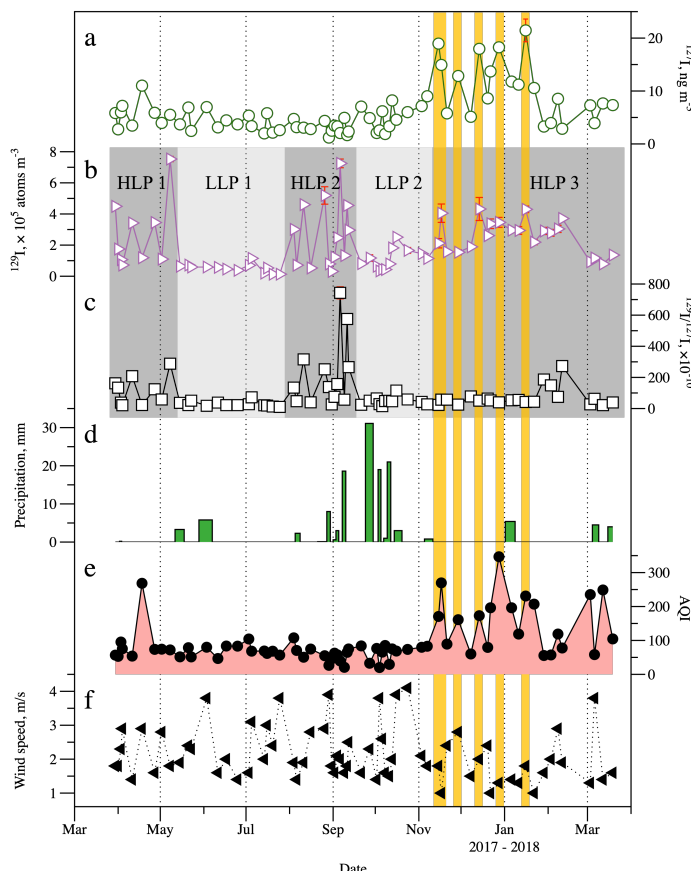
95 Fig.1 Map showing the sampling location (Xi'an city in rectangle) and East Asian monsoon (EAM) system. The inset shows the topography of the studied area in the Guanzhong Basin between the Loess Plateau to the north and Qinling Mountains to the south. East Asian monsoon, constituted by East Asian summer monsoon (EASM) and East Asian winter monsoon (EAWM), is one of vital components of the global atmospheric circulation system. The pink line in the map is the modern monsoon boundary, and the arrows indicate the westerly (orange), the EAWM (blue) and the EASM (red).

**Deleted:** Sixty eight  
**Deleted:** combing  
**Formatted:** Justified, Line spacing: 1.5 lines  
**Moved (insertion) [2]**  
**Deleted:** .  
**Deleted:** and a  
**Moved up [2]:** The sample collection and preparation procedure are described in detail in the supplementary information (SI-1).  
**Deleted:** , as previously reported (Zhang et al., 2018b)  
**Deleted:** s  
**Deleted:** of the iodine carrier are  
**Deleted:** determined to be  
**Deleted:** was less than  
**Deleted:** ... [1]  
**Formatted:** (Asian) Chinese (China), (Other) English (US)

**Deleted:** ping  
**Deleted:** n  
**Deleted:** .  
**Formatted:** Caption  
**Deleted:** and  
**Deleted:** (a)  
**Deleted:** China, (b) Xi'an city  
**Deleted:** (EAM)  
**Deleted:** upper panel  
**Deleted:** show  
**Deleted:** ¶

125 **3 Results**

Results of  $^{127}\text{I}$  and  $^{129}\text{I}$  concentrations,  $^{129}\text{I}/^{127}\text{I}$  atomic ratio, in aerosol samples in Xi'an, China from March 2017 to March 2018, are shown in Fig. 2. Concentrations of  $^{127}\text{I}$  and  $^{129}\text{I}$  and  $^{129}\text{I}/^{127}\text{I}$  atomic ratios fell within  $1.21\text{--}21.4 \text{ ng m}^{-3}$ ,  $(0.13\text{--}7.53) \times 10^5 \text{ atoms m}^{-3}$ , and  $(10.6\text{--}743) \times 10^{-10}$ , respectively. The mean values were  $6.22\pm4.48 \text{ ng m}^{-3}$ ,  $(4.97\pm1.65) \times 10^5 \text{ atoms m}^{-3}$ , and  $(92.7\pm124) \times 10^{-10}$  for  $^{127}\text{I}$ ,  $^{129}\text{I}$  concentrations and  $^{129}\text{I}/^{127}\text{I}$  atomic ratios, respectively.



130

Formatted: English (US)

Deleted: n

Deleted: and Table S1 in Supporting Information

Deleted: in aerosol samples from Xi'an

Deleted:  $\mu$ Deleted:  $\mu\text{g}$ 

Deleted: 2.22

Deleted: 87

Deleted: 101

140 Fig.2 Temporal variation of  $^{127}\text{I}$  (a),  $^{129}\text{I}$  (b) and  $^{129}\text{I}/^{127}\text{I}$  ratios (c) in aerosol samples collected in Xi'an, China from March 2017 to March 2018. The meteorological and air quality data includes precipitation (d), Air quality index (AQI, e) and wind speed (f). Orange bands indicate five heavy haze episodes corresponding with five  $^{127}\text{I}$  peaks. Three dark and two light grey shades in b and c demonstrate the high-level and low-level periods (HLP and LLP), respectively, for  $^{129}\text{I}$  and  $^{129}\text{I}/^{127}\text{I}$  ratios, alternatively dominated by the EAWM and EASM, respectively.

145  $^{127}\text{I}$  and  $^{129}\text{I}$  in aerosols are characterized with apparently monthly and seasonal variations (Fig.3 and 4). The minimum and maximum of monthly concentrations were observed in August and December for  $^{127}\text{I}$ , and July and December for  $^{129}\text{I}$ , respectively. The average  $^{127}\text{I}$  concentrations in November, December and January ( $11.4\pm12.7 \text{ ng m}^{-3}$ ) were two times higher than in other months ( $3.12\pm6.70 \text{ ng m}^{-3}$ ). Distinct from  $^{127}\text{I}$ , monthly variation of  $^{129}\text{I}$  shows the lowest level in June and July ( $(0.47\pm0.50)\times10^5 \text{ atoms m}^{-3}$ ), about two to six times lower than the other months. The maximum of  $^{129}\text{I}/^{127}\text{I}$  ratio was not observed in winter months but in September.

150 The average  $^{127}\text{I}$  concentrations were  $5.68\pm2.24 \text{ ng m}^{-3}$ ,  $3.61\pm1.49 \text{ ng m}^{-3}$ ,  $6.05\pm4.52 \text{ ng m}^{-3}$ , and  $10.6\pm6.0 \text{ ng m}^{-3}$  in spring, summer, fall and winter, respectively. The level of  $^{127}\text{I}$  in winter was about two times higher than spring and fall, three times higher than summer.  $^{129}\text{I}$  were  $(1.93\pm1.90)\times10^5 \text{ atoms m}^{-3}$ ,  $(1.17\pm1.55)\times10^5 \text{ atoms m}^{-3}$ ,  $(1.92\pm1.62)\times10^5 \text{ atoms m}^{-3}$ , and  $(3.12\pm0.72)\times10^5 \text{ atoms m}^{-3}$  in spring, summer, fall and winter, respectively. The level of  $^{129}\text{I}$  in winter was about two times 155 higher than spring and fall, and 3.3 times higher than summer. Seasonal variation of  $^{129}\text{I}/^{127}\text{I}$  ratios was not such obvious as the concentrations of iodine isotopes. The mean  $^{129}\text{I}/^{127}\text{I}$  ratio of  $(119\pm185)\times10^{-10}$  in fall were slightly higher than those of  $(82.2\pm79.3)\times10^{-10}$  in spring,  $(71.5\pm89.3)\times10^{-10}$  in summer and  $(89.3\pm70.5)\times10^{-10}$  in winter. Whereas, the ratios in all four seasons fell in the similar range as that of the whole year.

**Deleted:**  $^{127}\text{I}$  and  $^{129}\text{I}$  in aerosols are characterized with the apparent monthly and seasonal variations, which are described in SI-1 and SI-2 in detail (Fig.S1 and S2). In general, the concentrations of  $^{127}\text{I}$  and  $^{129}\text{I}$  are found highest in winter with maximum in December and September, respectively, and lowest in summer with minimum in August and July, respectively, and in between for spring and fall.

**Formatted:** (Asian) Chinese (China), (Other) English (US)

**Formatted:** Not Highlight

**Formatted:** (Asian) Chinese (China), (Other) English (US)

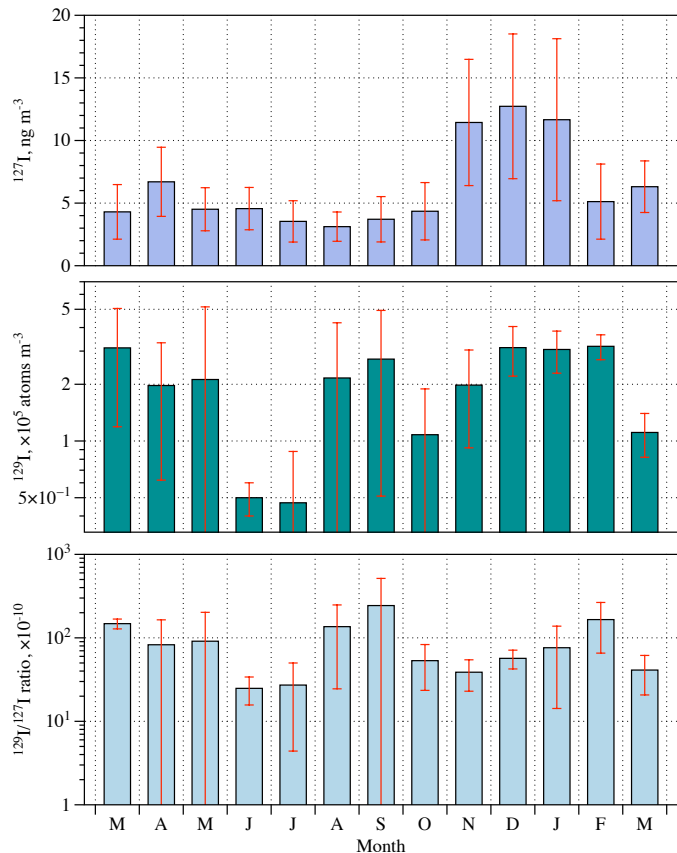


Fig. 3 Monthly variation of  $^{127}\text{I}$  (a),  $^{129}\text{I}$  concentrations (b) and  $^{129}\text{I}/^{127}\text{I}$  ratios (c) in aerosols from March 2017 to March 2018<sub>a</sub>

**Formatted:** Justified, Level 2, Space After: 10 pt, Line spacing: single

**Formatted:** Font: 9 pt, Bold

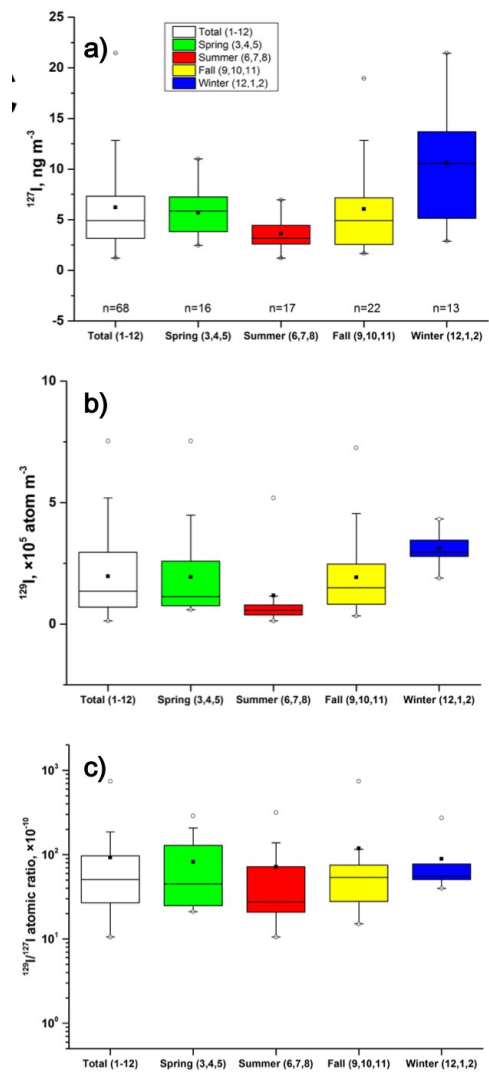


Fig. 4 Seasonal variation of  $^{127}\text{I}$  (a),  $^{129}\text{I}$  (b) and  $^{129}\text{I}/^{127}\text{I}$  atomic ratios (c) in aerosols collected in Xi'an, China from March 2017 to March 2018. The boxes show the range from 25% to 75%. Mean and median values are indicated with black solid squares and horizontal bars, respectively. The whisker indicates the upper and lower limits excluding outliers shown by dots. The outliers are defined as those 1.5 times greater than the interquartile range.

A weak correlation between  $^{129}\text{I}$  and  $^{127}\text{I}$  was found with Spearman correlation coefficient of 0.33 ( $p < 0.01$ ) for the whole year data, while no significant correlation between the two iodine isotopes in each season at the level of 0.05 (Table 1 and Fig. S1).

The correlation analysis between iodine isotopes and total suspended particle (TSP) indicate that there was a strong correlation between  $^{127}\text{I}$  and TSP, while no correlation between radioactive  $^{129}\text{I}$  and TSP (Fig. S2).

#### 4 Discussion

##### 4.1 Level and sources of $^{127}\text{I}$ and $^{129}\text{I}$

The results of a weak correlation in the whole year sampling and no significant correlations in each season between the two isotopes indicate that  $^{127}\text{I}$  and  $^{129}\text{I}$  have different sources and influence factors.

###### 180 4.1.1 $^{127}\text{I}$

The level of  $^{127}\text{I}$  concentrations, in particular in winter, is much higher than those in continental sites (below 0.61  $\text{ng m}^{-3}$  in South Pole and 2.7-3.3  $\text{ng m}^{-3}$  in the Eastern Transvaal), and comparable to those in coastal and ocean sites (typically below 20  $\text{ng m}^{-3}$ , and up to 24  $\text{ng m}^{-3}$  in tropic marine aerosols) (Saiz-Lopez et al., 2012). A similar range of  $^{127}\text{I}$  in TSP was observed to be 4.5-22  $\text{ng m}^{-3}$  at a coastal urban, Shanghai, China, showing lowest in summer and an increase occurred in fall and winter

185 (Gao et al., 2010). Iodine associated with PM10 and PM2.5 were found to be 3.0-115  $\text{ng m}^{-3}$  and 4-18  $\text{ng m}^{-3}$ , respectively, in urban and island sites of Shanghai, slightly lower than TSP iodine (Cheng et al., 2017; Gao et al., 2010). The marine aerosol iodine offshore China was found below 8.6  $\text{ng m}^{-3}$  during the XueLong cruise from July to September 2008 (Xu et al., 2010).

The results suggest a relatively high aerosol  $^{127}\text{I}$  level in both inland and coastal urbans in China.

Natural iodine in air is from marine emission through sea spray, weathering of base rock and continental release through 190 vegetation and suspended soil particles (Carpenter et al., 2013; Fuge and Johnson, 1986). Due to the influence of southeasterly EASM, moisture from the Pacific Ocean and the Chinese seas might bring marine iodine. Whereas, the mean  $^{127}\text{I}$  concentration in summer aerosol is  $3.61 \pm 1.49 \text{ ng m}^{-3}$ , about three-fold lower than that in winter. The sampling location, Xi'an, is an inland city about 900 km away from the nearest coastline. The contribution of marine iodine to terrestrial surface system in winter is considered to be negligible when the site is over 400 km away from the ocean (Cohen, 1985). Taking sodium and calcium as reference elements for sea spray and direct volatilization of iodine from the ocean and weathering of soil and rock, respectively, He et al. (2012) has been estimated that less than 0.04% and 5.2% of iodine were from direct marine contribution and weathering of soil and rock, respectively, to the precipitation at Zhouzhi county, Xi'an city (He, 2012). Despite being likely underestimated, marine iodine contribution in precipitation samples showed a decline trend with increasing distance of 20 km

**Deleted:** a Pearson

**Formatted:** Not Highlight

**Deleted:** 34 ...3 ( $p =$  ... [2]

**Formatted:** Font: (Default) Times New Roman

**Deleted:** 01...1) for the whole year data, while no significant correlation between the two iodine isotopes in each season at the level of 0.05 (Table 1 and Fig. S3...1). The correlation analysis between iodine isotopes and total suspended particle (TSP) indicate that there was a strong correlation between  $^{127}\text{I}$  and TSP, while no correlation between radioactive  $^{129}\text{I}$  and TSP (Fig. S4 ... [3]

**Formatted:** English (US)

**Deleted:** Although ... weak correlation was observed between  $^{127}\text{I}$  and  $^{129}\text{I}$  ...n the whole year sampling, there were ... [4]

**Formatted:** Not Highlight

**Deleted:** in each season,...indicating ... [5]

**Deleted:** terrestrial air ...ontinental sites (below 0.61  $\text{ng m}^{-3}$  in South Pole 1  $\text{ng m}^{-3}$ ...nd 2.7-3.3  $\text{ng m}^{-3}$  in the Eastern Transvaal), and also slightly higher...omparable than ...o those in coastal and marine air...cean sites (< 10...pically below 20  $\text{ng m}^{-3}$ , and up to 24  $\text{ng m}^{-3}$  in tropic marine aerosols) (Saiz-Lopez et al., 2012). Whereas, a... similar range of  $^{127}\text{I}$  in TSP was observed to be 4.5-22  $\text{ng m}^{-3}$  at a coastal urban, and Shensi Island of ...hanghai, China, showing, ... [6]

**Formatted** ... [7]

**Deleted:** This ...he results suggests...that ... relatively higher...aerosol  $^{127}\text{I}$  level in aerosols ...n both inland and coastal cities ... ... [8]

**Formatted:** English (US)

**Deleted:** Iodine in urban air generally origins from natural and anthropogenic sources ...atural iodine in air is from marine emission through sea spray, weathering of base rock and continental release through vegetation and suspended soil particles (Carpenter et al., 2013; Fuge and Johnson, 1986). Due to the influence of southeasterly EASM, moisture from the Pacific Ocean and the Chinese seas might bring oceanic ...rine iodine. Whereas, the mean  $^{127}\text{I}$  concentration in summer aerosol is  $3.61 \pm 1.49 \text{ ng m}^{-3}$ , about three-fold lower than that in winter. The sampling location, Xi'an, is an inland city about 900 km away from the nearest coastline. The contribution of oceanic marine iodine to terrestrial surface system in winter is considered to be negligible when the site is over 400 km away from the ocean (Cohen, 1985). Taking sodium and calcium as reference elements for sea spray and direct volatilization of iodine from the ocean and weathering of soil and rock, respectively, He et al. (2012) has been estimated that less than 0.04% and 5.2% of iodine were from direct the ...rine direct ...ontribution of ocean ... [9]

**Formatted** ... [10]

to 1252 km from the sea. And no significant change of marine contribution could be found over 100 km from the sea (He, 2012).

Iodine is also emitted from volatility of terrestrial soil and respiration of vegetation, which was estimated to be  $2.27 \mu\text{g m}^{-2} \text{d}^{-1}$  in the form of  $\text{CHI}_3$  on a global basis, over an active season of 240 days, together with biome areas for temperate forest and 275 wood lands ( $28.5 \times 10^{12} \text{ m}^2$ ) and temperate grasslands ( $31.9 \times 10^{12} \text{ m}^2$ ) (Sive et al., 2007). Dry deposition flux of iodine, however, can be calculated to be  $5.83-40.7 \mu\text{g m}^{-2} \text{d}^{-1}$  based on aerosol  $^{127}\text{I}$  mass concentrations in TSP ( $13.3-92.5 \mu\text{g g}^{-1}$  TSP), multiplying an annual average dustfall flux of  $13.2 \text{ t (km}^2 \text{ 30 d}^{-1}$ ) (Xi'an Bureau of Statistics, 2018). The uncertainty for the calculation is about 32% mainly due to the large uncertainty of dustfall flux of about 31%. Because of different land coverage between urban and forest-grassland in reference of Sive et al. (2007), terrestrial emission of iodine in the sampling site should be even lower 280 than  $2.27 \mu\text{g m}^{-2} \text{ d}^{-1}$ . The dry deposition flux of iodine in Xi'an was therefore far beyond terrestrial sources of soil and vegetations, indicating they might be important iodine sources in summer, but not in winter.

The significant increase of  $^{127}\text{I}$  from summer to winter suggests that anthropogenic discharge of iodine is the dominant source of  $^{127}\text{I}$  in Xi'an aerosol samples, mainly including combustion of biomass and fossil fuel (Wu et al., 2014). Biomass combustion generally occurs in summer harvest time, normally in later May and early June. In order to improve air quality, Xi'an 285 government has banned biomass combustion since 2009. Additionally, no obvious change in  $^{127}\text{I}$  concentrations was found in May and June, indicating the biomass combustion is not the major source.

A recent study has confirmed that particulate iodine around two coal plants in Nanchang city, China, was greatly increased up to  $36 \text{ ng m}^{-3}$ , and iodine concentrations within 9 km from the coal plants were much higher than that in non-coal sites (Duan, 2018). Coal is dominant in energy consumption structure. Coal consumption accounts for 72.7% of total energy consumption 290 in Shaanxi province in 2013. In 2017, the coal consumption in Guanzhong basin is 67.4 million tons (Shaanxi Provincial Bureau of Statistics, 2018).  $^{127}\text{I}$  concentration in coal produced in Shaanxi province ranges from 0.39 to  $6.53 \mu\text{g g}^{-1}$  with a mean value of  $1.47 \mu\text{g g}^{-1}$  (Wu et al., 2014). An atmospheric iodine emission factor that equals to the ratio of the iodine released into the atmospheric from the coal is from 78.8% to 99.4%, depending on the coal combustion technology and emission control devices (Wu et al., 2014). If simply assuming anthropogenic iodine is solely from combustion of coal in the study area and the 295 atmospheric iodine emission factor is 92%, about 91 tons of  $^{127}\text{I}$  can be released to the atmosphere in the Guanzhong Basin in 2017. Xi'an, a northern city in China, consumes more coals in the heating period from November 15 to March 15, which aggravates iodine release from coal combustion. Thus, we suggest that coal combustion is the major source of  $^{127}\text{I}$  in Xi'an urban aerosols in particular during the heating period of winter. This also suggests that  $^{127}\text{I}$  was regionally or locally input, and can be treated as internal release.

#### 300 4.2.2 $^{129}\text{I}$

The aerosol  $^{129}\text{I}$  levels reported in the previous studies and this work could be categorized into three groups (Fig. 5). 1) Compared to other investigating sites, aerosol  $^{129}\text{I}$  concentrations were less than  $10^6 \text{ atoms m}^{-3}$  in Xi'an, northwest China. This low level is also found at those sites remote from the nuclear facilities in southern and central Europe, as well as Japan before

**Formatted:** English (US)

**Formatted:** Font color: Text 1

**Formatted:** Font: 10 pt, Font color: Text 1

**Formatted:** Font color: Text 1

**Formatted:** Font color: Text 1

**Deleted:** 8.78

**Deleted:** 39.6

**Formatted:** Superscript

**Deleted:** in this study and

**Deleted:**

**Deleted:** from the "2017 Xi'an Environmental bulletin"

**Deleted:** iodine

**Deleted:** es

**Deleted:** major

**Formatted:** (Asian) Chinese (China), (Other) English (US)

**Formatted:** English (US)

**Moved down [1]:** Coal consumption accounts for 72.7% of total energy consumption in Shaanxi province in 2013.

**Formatted:** Font color: Text 1

**Moved (insertion) [1]**

**Deleted:** our

**Deleted:** The area of the Guanzhong Basin is  $3.6 \times 10^4 \text{ m}^2$ , and the height of troposphere is taking as 10 km. Then,  $^{127}\text{I}$  concentration in the air is about  $25 \text{ ng m}^{-3}$ . The particle-associated iodine accounts for approximately 10%-20% (Hasegawa et al., 2017). Thus,  $^{127}\text{I}$  in aerosols can be estimated to be about  $25-50 \text{ ng m}^{-3}$ . The estimated value is comparable with the  $^{127}\text{I}$  peak values in winter, but about ten times higher than the less polluted aerosol  $^{127}\text{I}$  concentrations ( $1.21-9.01 \text{ ng m}^{-3}$ ).

**Deleted:** the

**Deleted:** ed

**Deleted:** , and more than 60% of coal-derived iodine has been dispersed out of the Guanzhong Basin

**Formatted:** (Asian) Chinese (China), (Other) English (US)

**Formatted:** Line spacing: 1.5 lines

**Deleted:** 3

**Deleted:**  $10 \times 10^5$

the Fukushima accident (Hasegawa et al., 2017; Jabbar et al., 2013; Santos et al., 2005). The lowest  $^{129}\text{I}$  ( $< 0.1 \times 10^5$  atoms  $\text{m}^{-3}$ ) in aerosols have been found at two high altitude sites of Alps mountains (about 3000 m above the sea level). 2) The high values beyond  $10^8$  atoms  $\text{m}^{-3}$  have been reported at the sites directly contaminated either by nuclear reprocessing plants, such as Hanford, Sellafield and WAK at Karlsruhe, or by Fukushima nuclear accident in 2011 (Brauer et al., 1973; Jackson et al., 2002; Wershofen and Aumann, 1989; Xu et al., 2015). 3) In between, aerosol  $^{129}\text{I}$  within the range from  $10^6$  atoms  $\text{m}^{-3}$  to  $10^8$  atoms  $\text{m}^{-3}$ , are mainly found in the sites and periods with global fallout from atmospheric nuclear weapon testing, and indirectly 335 contaminations from nuclear fuel reprocessing plants (Brauer et al., 1973; Englund et al., 2010; Kadowaki et al., 2018; Tsukada et al., 1991; Zhang et al., 2016). ▼

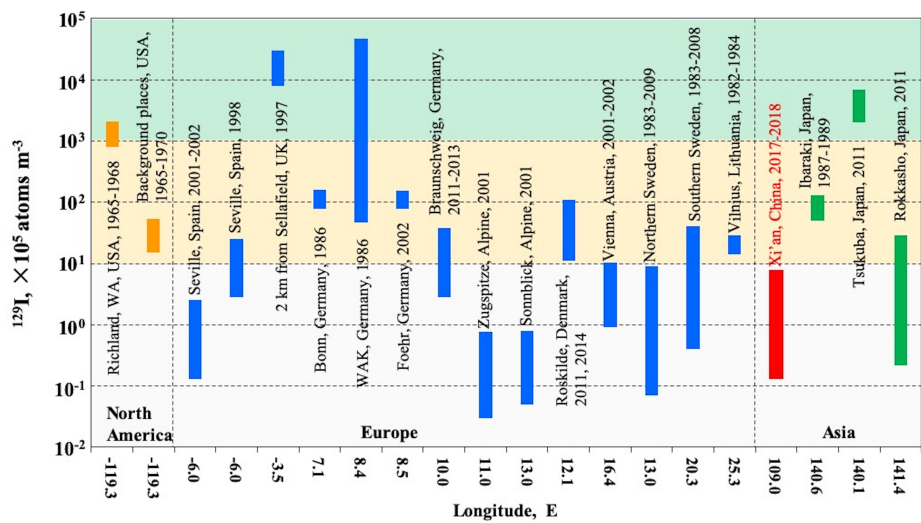
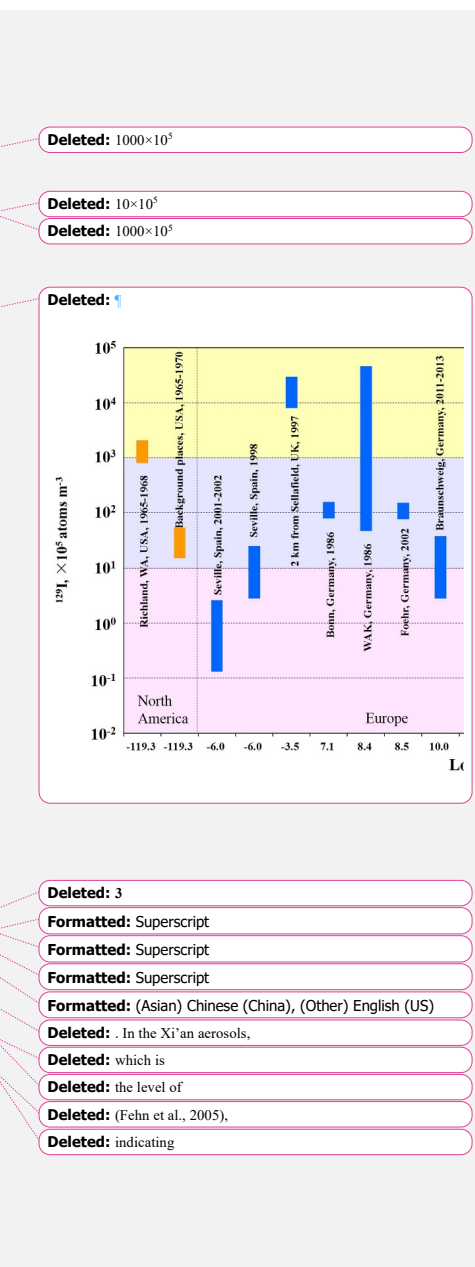


Fig. 5 Comparison of aerosol  $^{129}\text{I}$  levels in Xi'an, China (red bars) with other investigations in North America (orange), Europe (blue) and East Asia (Green) distributed by longitude. The green, yellow and white bands are high ( $> 10^8$  atoms/ $\text{m}^{-3}$ ), middle ( $10^6$  to  $10^8$  atoms/ $\text{m}^{-3}$ ) and low ( $< 10^6$  atoms/ $\text{m}^{-3}$ )  $^{129}\text{I}$  concentrations in aerosols.

The source term of  $^{129}\text{I}$  is crucial for spatial and temporal distributions of  $^{129}\text{I}$  in global scale.  $^{129}\text{I}/^{127}\text{I}$  atomic ratios in the Xi'an aerosols range from  $10.6 \times 10^{-10}$  to  $743 \times 10^{-10}$ , at least three orders of magnitude higher than naturally produced  $^{129}\text{I}$  level ( $1.5 \times 10^{-12}$ ) (Fehn et al., 2005). This clearly indicates human nuclear activities are dominant contributor for the increase of  $^{129}\text{I}$  level in the environment. The level and source of  $^{129}\text{I}$  in soil, vegetation, rain and rivers water samples have been previously 345 investigated in Xi'an region, where  $^{129}\text{I}/^{127}\text{I}$  varied from  $1.1 \times 10^{-10}$  to  $43.5 \times 10^{-10}$  with a mean value of  $20.6 \times 10^{-10}$  (Zhang et al., 2016).



al., 2011). Aerosol  $^{129}\text{I}/^{127}\text{I}$  ratios were about one order of magnitude higher than those in other environmental media, indicating  $^{129}\text{I}$  in Xi'an aerosols was not released by local soil suspension and vegetation release. Weathering of bed rock is neither a major source of airborne  $^{129}\text{I}$ , since weathering just contributes 5% of stable iodine, and  $^{129}\text{I}$  in bed rock can be considered even lower than the nature-produced  $^{129}\text{I}$  level because of the continuous decay. Coal combustion contributes a large proportion of stable  $^{127}\text{I}$  in winter, while  $^{129}\text{I}$  amount in coals is almost negligible, because coal was formed in Tertiary (2.58-66 million years) at the latest so that  $^{129}\text{I}$  has been decayed out or in an extremely low value of  $10^{-13}\text{--}10^{-10}$  for  $^{129}\text{I}/^{127}\text{I}$ . Thus, coal combustion is not a major source of atmospheric  $^{129}\text{I}$ .

360 365 Nuclear activities including the historic nuclear weapon testing sites, nuclear reactors, NFRPs in China and Europe, as well as the underground nuclear weapon testing are considered. Two nuclear weapon testing sites, Semipalatinsk and Lop Nor, locating upwind, may input  $^{129}\text{I}$  into Xi'an region through soil resuspension and gaseous re-emission. However, evidence from  $^{129}\text{I}$  distribution in surface soils from upwind regions reveals that the two nuclear weapon testing sites has limit impact on the atmospheric  $^{129}\text{I}$  level in the remote regions farther than 1000 km from these test sites (Fan, 2013). This is also supported by 370 the back-trajectory analysis that  $^{129}\text{I}$  concentration did not significantly raised when abundant air masses from Xinjiang passing through the Lop Nor test site on December 28, 2018 (Fig. S3g). Five nuclear power plants are in operation along the southeast coastal areas in China.  $^{129}\text{I}$  data in sea water collected within 10 km from a Chinese nuclear power plant suggests that normal operation of reactors does not have significant increase in  $^{129}\text{I}$  concentrations (He et al., 2011). Although information on gaseous release of  $^{129}\text{I}$  from these reactors is unknown, the low  $^{129}\text{I}/^{127}\text{I}$  (about  $7\times10^{-10}$ ) in the surface soil of southern China

375 380 385 (Guangxi, Jiangxi and Fujian Provinces) close to the reactors can confirm that there is no marked deposition from the gaseous release (Fan, 2013). Toyama et al. (2013) have shown a direct close-in influence of a pilot plant in Tokaimura (Ibaraki Prefecture), Japan on the  $^{129}\text{I}$  deposition in Tokyo. Similarly, a pilot nuclear spent fuel reprocessing plant (NFRP) has been established and operated in Gansu province, China since 2010. This NFRP is locating in an upwind area and about 1200 km northeast of Xi'an. During the sampling period in 2017/2018, no abnormally high  $^{129}\text{I}$  was observed, while this contribution cannot be neglected in the future operation, and should be continuously monitored. In addition, the possible influence of the sixth underground nuclear weapon test conducted by North Korea on September 3, 2017 has been excluded based on the back and forward trajectories and the nuclear environmental monitoring around the Chinese northeast border by the government (Ministry of Environmental Protection of the People's Republic of China, 2017).

It is well documented that gaseous and liquid discharges from the NFRPs in Sellafield, United Kingdom and La Hague, France, 390 as well as the secondary emission from the contaminated seas and land, are the predominant source of  $^{129}\text{I}$  in the modern atmosphere, in particular in European environment (Jabbar et al., 2013). The two NFRPs are located in the  $50\text{--}55^\circ\text{N}$ , the westerly belt. The prevailing westerly winds throughout the year in the mid-latitude act as a crucial pathway of  $^{129}\text{I}$  transport from its source to the whole mid-latitude regions of the northern hemisphere, as observed in the sediment core from Jiaozhou Bay, east coast of China (Fan et al., 2016). The 60-year record of  $^{129}\text{I}$  in a lacustrine sediment from Philippines further shows that the EAWM plays an important role in transporting the mid-latitude  $^{129}\text{I}$  to the low-latitude regions (Zhang et al., 2018a). The feature of  $^{129}\text{I}$  variation also shows that  $^{129}\text{I}$  was in high level in spring and winter when EAWM prevailing and low level

**Deleted:** in aerosols

**Deleted:** samples

**Formatted:** Superscript

**Formatted:** Superscript

**Formatted:** Superscript

**Deleted:** nuclear spent fuel reprocessing plant (

**Deleted:** )

**Deleted:** S5g

**Field Code Changed**

**Deleted:** (2012)

**Deleted:** (Toyama et al., 2013)

**Deleted:** nuclear fuel reprocessing plants (

**Deleted:** )

in summer when EASM prevailing, supporting that the  $^{129}\text{I}$  is dominantly sourced from the long-range transport of European NFRPs discharges. In this case,  $^{129}\text{I}$  is externally input ~~in contrast to the~~ locally released stable  $^{127}\text{I}$ .

**Deleted:** relative

#### 4.2 Factors influencing temporal variation of iodine isotopes

As discussed above, even though variation pattern of  $^{127}\text{I}$  and  $^{129}\text{I}$  were similar, they were considerably influenced by many factors owing to their different sources. In this work, meteorological factors including precipitation, wind speed, temperature and dust storm events, atmospheric circulation (in particular EAM), heavy air pollution periods are discussed.

##### 4.2.1 Meteorological factors

**Precipitation and wind speed.** As discussed in supplementary information (SI 2), the influences of precipitation and wind speed on temporal changes of iodine isotopes are not significant (Fig. 2e and 2f). However, the winter days with absence of wet precipitation and lower wind speed well corresponded to the heavy haze episodes when iodine concentrations, in particular stable  $^{127}\text{I}$ , were greatly increased, indicative of less dispersion. The details about haze influence on iodine will also be discussed in the ~~following~~ section.

**Deleted:** 3

**Temperature.** Temperature and its associated physiochemical processes and biological release of iodine from source regions might be a reason for the variation patterns. In summer, the temperature is ~~about~~ 20-40°C in ~~North~~ hemisphere, which 415 is favourable for direct volatilization of iodine from the surfaces of land and seas. Ozone in air-sea boundary layer is suggested to act as an oxidants to transform iodide in seawater to volatile molecular iodine that enters into the air, which is believed more significant than the biological process (Carpenter et al., 2013). Ozone concentrations in summer is around 30 ppb, roughly 420 two times higher than winter (Ayers et al., 1996), which may increase ~~re~~-emission rate of iodine from the ocean and  $^{129}\text{I}$ -contaminated sea surface into the air. Additionally, the bloom of phytoplankton and algae in summer, can release biogenic organic iodine into the air through a mechanism of anti-oxidation (Küpper et al., 2008). The temperature, ozone concentration 425 and marine biomass greatly reduces in winter, which will result in less iodine released from the source regions, and can be used to explain the relatively weak peaks in winter than in summer. As discussed above,  $^{127}\text{I}$  and  $^{129}\text{I}$  in Xi'an aerosols were mainly derived from coal combustion and long-range transport from Europe, ~~respectively~~. The change in release amount of  $^{127}\text{I}$  and  $^{129}\text{I}$  at the source regions is obviously not the determining factor for the changes of iodine isotopes since Xi'an is far 430 from the oceans and the  $^{129}\text{I}$  source regions. Furthermore, the seasonal variation of  $^{127}\text{I}$  and  $^{129}\text{I}$  with low level in summer can also easily exclude the possibility of temperature influence.

**Deleted:** other

**Deleted:** following

**Deleted:** from

**Deleted:** the n

**Deleted:** t

**Deleted:** the

**Dust storm.** Two severe dust storm events occurred in Xi'an in 17-18 April and 4-6 May, 2017, as ~~indicated~~ by the peaks of air quality index (AQI) of 268 and 306, respectively. A  $^{127}\text{I}$  peak,  $11.0 \text{ ng m}^{-3}$ , was observed on 18 April, 2017, while  $^{127}\text{I}$  levels in other samples were almost below  $6 \text{ ng m}^{-3}$  in spring and summer time. Dust storms frequently occur in winter and 430 spring in north China, and normally originate from the arid and semi-arid desert regions mainly locating in Mongolia and northwest China. The first dust storm arrived the Guanzhong basin on 17 April 2017, and lasted until 19 April (China Meteororological Administration, 2017). The small peak of  $^{127}\text{I}$  is likely attributed to the suspended particulate matter from

**Deleted:** shown

**Deleted:** (Fig. 2e)

the soil surface in the dust storm source. In contrast, variation of  $^{129}\text{I}$  level did not reflect the dust storm influence. The fact that  $^{129}\text{I}$  was not correlated with particulate concentrations (Fig. S4), indicates that the extrinsic  $^{129}\text{I}$  is not related to the heavy 445 particulate events, since the major dust source areas include Taklimakan desert, the Gobi Desert in Inner Mongolia, and the Loess Plateau, where the  $^{129}\text{I}/^{127}\text{I}$  ratios in surface soil fell below  $60 \times 10^{-10}$ , apparently much lower than those in aerosols (Zhang et al., 2011). Furthermore, the back-trajectory analysis also showed that the low  $^{129}\text{I}$  level on April 18 can be partially attributed to an  $^{129}\text{I}$ -poor low-altitude air mass (< 900 m) (Fig. S3a). This is because either the low-altitude air mass might be formed in 450  $^{129}\text{I}$ -poor inland areas, not from the  $^{129}\text{I}$ -rich European area, or long-range transported  $^{129}\text{I}$  in low-altitude air mass could be easily lost by the topographic countercheck (Dong et al., 2018).

The second dust storm has started from the south-central Mongolia and the west-central Inner Mongolia autonomous region since 3 May, arrived at Xi'an on 5 May and retreated on 6 May. It is pity that no sample was analysed in this event, but a significant  $^{129}\text{I}$  peak with value of  $7.53 \times 10^5$  atoms  $\text{m}^{-3}$  was found after three days of this event (Fig. 2b). The back-trajectory analysis suggests the  $^{129}\text{I}$  peak on May 8, 2017 is found to relate to the downdraft originated from high altitude (2000–6000 m) 455 to low altitude (500 m) (Fig. S3b). This elevation of  $^{129}\text{I}$  after the dust storm events is likely attributed that the intensified winter monsoon and strong cold high pressure transporting greater  $^{129}\text{I}$  from Europe to China.

#### 4.2.2 Heavy haze episodes during 2017/2018 winter

A significantly positive correlation between  $^{127}\text{I}$  and air quality index (AQI) was found with a high Spearman correlation coefficient of 0.72 ( $p < 0.05$ ) for the whole-year sampling period, and an increased coefficient of 0.87 in winter (Table 1). The 460  $^{127}\text{I}$  concentration in winter can reach up to 10 times as much as in summer (Fig. 2a). Furthermore, five  $^{127}\text{I}$  peaks from 12.8 to 21.4 ng  $\text{m}^{-3}$  were clearly identified on 15 and 29 November, 14 and 28 December, and 16 January, respectively, which well coincided with the heavy haze episodes with AQI mostly over 200, namely heavily polluted air (Fig. 2e). As discussed in section 4.1, the irrelevance between  $^{127}\text{I}$  and  $^{129}\text{I}$  in aerosols for each season attributed to their different sources, also demonstrates that locally discharged iodine and externally input iodine are not contemporaneously subjected to formation of iodine-containing particles. 465

Further analysis showed close relationship between  $^{127}\text{I}$  and six air pollutants, including PM 10, PM 2.5, CO,  $\text{SO}_2$ ,  $\text{NO}_2$  and  $\text{O}_3$  (Table 1 and Fig. S4). In spring and summer, the high correlation between  $^{127}\text{I}$  and AQI can be attributed to the high correlation between  $^{127}\text{I}$  with PM10 and PM2.5. In fall and winter,  $^{127}\text{I}$  is significantly positively correlated with PM 10, PM 2.5, CO,  $\text{SO}_2$  and  $\text{NO}_2$ , and negatively correlated with  $\text{O}_3$ . In contrast, there is no such good agreement between  $^{129}\text{I}$  and these 470 gaseous pollutants. Despite that, three  $^{129}\text{I}$  peaks were found on 15 November, 14 December, 2017 and 16 January 2018, respectively, which well corresponded with high  $^{127}\text{I}$  concentrations (Fig. 2a and 2b) during the haze episodes. This reflects that the formation mechanism of iodine-containing aerosols might be seasonally different. However, the three peaks of  $^{129}\text{I}$  in aerosols during the heavy haze episodes suggest that local and external iodine are likely subjected to subsequent growth of particles and capture by particles due to a longer residence time in stagnant weather conditions.

**Deleted:** Meantime ... furthermore, the back trajectory ... [11]  
**Formatted** ... [12]  
**Deleted:** S5a  
**Formatted** ... [13]  
**Deleted:** .  
**Formatted:** English (US)  
**Deleted:** back trajectory ...ack-trajectory analysis suggests the  $^{129}\text{I}$  peak on May 8, 2017 is found to relate to the downdraft originated from high altitude (2000–6000 m) to low altitude (500 m) (Fig. S5) [14]  
**Deleted:** Pearson  
**Formatted:** Not Highlight  
**Deleted:** 79  
**Formatted:** Not Highlight  
**Deleted:** 84 ... 7 in winter (Table 1). The  $^{127}\text{I}$  concentration in winter can reach to ...p to 10 times as much as in summer (Fig. 2a). Furthermore, five  $^{127}\text{I}$  peaks from 12.8 to 21.4 ng  $\text{m}^{-3}$  were clearly identified on 15 and 29 November, 14 and 28 December, and 16 January, respectively, which well coincided with the heavy haze episodes with AQI mostly over 200, namely heavily polluted air (Fig. 2e). As discussed in section 4.1, the irrelevance between  $^{127}\text{I}$  and  $^{129}\text{I}$  in aerosols for each season attributed to their different sources, also demonstrates that locally discharged iodine and externally input iodine are not contemporaneously subjected to formation of iodine-containing particles. Typically, new particle formation occurs in two distinct stages, i.e., nucleation to form a critical nucleus and subsequent growth of the freshly nucleated particle to a larger size (Zhang et al., 2015). It is widely accepted that iodine is involved into the formation of fine particles, and increasing investigations have been carried out in coastal and open sea areas (Saiz-Lopez et al., 2012). However, in megacities with severe air pollution, the role of iodine formation and development of heavy haze events is far not understood. Iodine-mediated particles were suggested to be formed from highly concentrated, localized pockets of iodine oxides as primary nucleation, and to rapidly grow by uptake of  $\text{H}_2\text{SO}_4$ ,  $\text{H}_2\text{O}$ ,  $\text{NO}_2$ , short chain dicarboxylic acids, gaseous iodine and other gaseous species (Saiz-Lopez et al., 2012). Winter urban air in Xi'an provides two requirements of sufficiently high iodine concentrations and the presence of high levels of aerosol nucleation precursors, such as  $\text{SO}_2$ ,  $\text{NH}_3$ , amines, and anthropogenic VOCs. ... [15]  
**Deleted:** S6...4). In spring and summer, the high correlation between  $^{127}\text{I}$  and AQI can be attributed to the high correlation between  $^{127}\text{I}$  with PM10 and PM2.5. In fall and winter,  $^{127}\text{I}$  is significantly positively correlated with PM 10, PM 2.5, CO,  $\text{SO}_2$  and  $\text{NO}_2$ , and negatively correlated with  $\text{O}_3$  (Pearson correlation coefficient = -0.60,  $p = 0.02$ ) ... [16]  
**Formatted:** Highlight  
**Deleted:** In spring and summer, iodine is probably associated with primary matter and secondary organic aerosols due to low level of air iodine and greatly increased artificial and biogenic VOCs (Feng et al., 2016). In fall and winter when the key aerosol nucleation ... [17]  
**Formatted:** English (US)  
**Deleted:** .  
**Formatted** ... [18]  
**Deleted:** .  
**Formatted** ... [19]

**Table 1. Spearman correlation coefficients between iodine isotopes and atmospheric pollutants and weather conditions \***

Correlation	Whole year				Spring (3-5)				Summer (6-8)				Fall (9-11)				Winter (12-2)			
	$^{127}\text{I}$		$^{129}\text{I}$		$^{127}\text{I}$		$^{129}\text{I}$		$^{127}\text{I}$		$^{129}\text{I}$		$^{127}\text{I}$		$^{129}\text{I}$		$^{127}\text{I}$		$^{129}\text{I}$	
	Spea	Sig.	Spea	Sig.																
$^{127}\text{I}$	<b>0.33</b>	<b>0.01</b>			-0.05	0.86			0.35	0.17			0.04	0.86			0.51	0.08		
$^{129}\text{I}/^{127}\text{I}$	-0.28	0.02	0.74	0.00	-0.64	<b>0.01</b>	0.77	<b>0.00</b>	-0.03	0.90	<b>0.87</b>	<b>0.00</b>	-0.65	<b>0.00</b>	0.60	<b>0.00</b>	-0.94	<b>0.00</b>	-0.35	0.25
Temp	-0.53	<b>0.00</b>	-0.47	<b>0.00</b>	-0.09	0.75	-0.21	0.44	-0.15	0.55	-0.37	0.14	-0.54	<b>0.01</b>	0.07	0.75	0.13	0.67	-0.19	0.53
Humidity	-0.06	0.64	-0.13	0.27	0.24	0.37	<b>-0.53</b>	<b>0.04</b>	-0.06	0.82	0.29	0.26	-0.45	<b>0.04</b>	-0.30	0.18	<b>0.69</b>	<b>0.01</b>	0.34	0.26
Wind speed	-0.19	0.13	-0.21	0.09	-0.08	0.76	-0.31	0.24	-0.09	0.73	0.02	0.95	0.05	0.81	0.14	0.54	-0.34	0.26	0.14	0.65
Precipitation	-0.14	0.25	-0.18	0.15	-0.04	0.88	-0.13	0.64	0.04	0.87	0.42	0.09	-0.29	0.19	-0.39	0.07	0.15	0.61	0.00	1.00
AOI	<b>0.72</b>	<b>0.00</b>	0.17	0.17	<b>0.95</b>	<b>0.00</b>	-0.05	0.85	<b>0.59</b>	<b>0.01</b>	-0.01	0.97	<b>0.56</b>	<b>0.01</b>	0.13	0.55	<b>0.87</b>	<b>0.00</b>	0.45	0.12
CO	<b>0.54</b>	<b>0.00</b>	0.20	0.11	<b>0.66</b>	<b>0.01</b>	0.19	0.49	0.17	0.52	<b>0.56</b>	<b>0.02</b>	0.46	0.03	-0.18	0.42	<b>0.85</b>	<b>0.00</b>	0.40	0.18
SO <sub>2</sub>	<b>0.60</b>	<b>0.00</b>	0.47	0.00	0.24	0.38	-0.14	0.59	0.37	0.15	0.22	0.40	<b>0.53</b>	<b>0.01</b>	0.26	0.25	0.48	0.10	0.26	0.38
NO <sub>2</sub>	<b>0.63</b>	<b>0.00</b>	0.42	0.00	0.45	0.08	0.00	0.99	0.13	0.61	0.27	0.30	<b>0.61</b>	<b>0.00</b>	0.08	0.74	<b>0.73</b>	<b>0.00</b>	0.14	0.64
Q <sub>i</sub>	-0.44	0.00	-0.33	0.01	-0.32	0.23	0.09	0.75	0.39	0.12	-0.37	0.15	-0.20	0.37	0.28	0.21	-0.64	0.02	-0.11	0.72
PM10	<b>0.71</b>	<b>0.00</b>	0.24	0.05	<b>0.84</b>	<b>0.00</b>	0.00	0.99	<b>0.74</b>	<b>0.00</b>	0.21	0.42	<b>0.51</b>	<b>0.02</b>	0.14	0.54	<b>0.84</b>	<b>0.00</b>	0.50	0.08
PM2.5	<b>0.75</b>	<b>0.00</b>	0.24	0.05	<b>0.94</b>	<b>0.00</b>	0.00	1.00	<b>0.76</b>	<b>0.00</b>	0.19	0.47	<b>0.45</b>	<b>0.03</b>	0.10	0.67	<b>0.85</b>	<b>0.00</b>	0.47	0.11

\* Spearman correlation coefficient is used. 2-tailed test of significance is used. Correlation significant at the 0.05 level is in bold.

Formatted: Centered, Level 3

Formatted: Font: Bold, (Asian) Chinese (China)

#### 4.2.3 Impact of EAM for long-range transport of $^{129}\text{I}$

Increasing evidence have suggested that the prevailing westerly and EAM system act as crucial driving forces and pathways for transport of the European NFRPs derived  $^{129}\text{I}$  from Europe to East Asia and even to low-latitude southeast Asia (Fan et al., 2016; Zhang et al., 2018a). Monthly variations of atmospheric  $^{129}\text{I}$  in Japan also showed a clear pattern with low  $^{129}\text{I}$  deposition in summer and high in winter, which is also attributed to the impact of EAM (Hasegawa et al., 2017; Kadokawa et al., 2018; Toyama et al., 2013). In this work, seasonal variation of  $^{129}\text{I}$  was identical to the observation in the previous studies (Toyama et al., 2013). However, the day-resolution variation patterns of  $^{129}\text{I}$  and  $^{129}\text{I}/^{127}\text{I}$  in Xi'an, distinct from monthly variation in Japan, showed three periods with high levels and two periods with low levels, indicating more complex influence of EAM in the typically continental monsoon climate city, Xi'an.

The whole-year time series can be divided into five periods with three high-level periods (HLP), a) from late March to early May (HLP 1), b) from middle August to early September (HLP 2), and c) from middle November, 2017 to late February, 2018 (HLP 3); as well as two low-level periods (LLP), d) from early May to middle August (LLP 1), and e) from middle September to early November, 2017 (LLP 2) (Fig.2b and 2c).  $^{129}\text{I}$  levels in the three HLPs fell within the range of  $(1.98\text{--}2.41) \times 10^5$  atoms m<sup>-3</sup>, which is 3-5 times higher than those during the two LLPs with  $(0.49\text{--}0.66) \times 10^5$  atoms m<sup>-3</sup> (Table S1). The relative standard deviation shows much higher variability during HLP 1 and 2 from 91% to 109% in contrast to the variability in other clusters less than 60%.

The significant difference between the HLPs and LLPs suggests the transportation process of  $^{129}\text{I}$  is obviously distinct. The westerly is a crucial driving force of  $^{129}\text{I}$  from the NFRPs point sources and their contaminated seas, and labelled by a high  $^{129}\text{I}$  level up to  $10^6$  for  $^{129}\text{I}/^{127}\text{I}$  ratio (Michel et al., 2012; Zhang et al., 2016) (Fig.1a). Due to interplay between westerly and EAWM (An et al., 2012), EAWM inherits the high  $^{129}\text{I}$  feature of  $10^7\text{--}10^9$  for  $^{129}\text{I}/^{127}\text{I}$  ratio in the long-distance transport process. Therefore, the HLP 1 and 3 was strongly affected by the EAWM prevailing from early September to early may in 2017. Compared to the violent fluctuation of  $^{129}\text{I}$  in spring (HLP1), the weak fluctuations of HLP 3 in winter might be attributed

Formatted: Line spacing: Multiple 1.15 li

Formatted: Font: (Default) Times New Roman

Formatted: English (US)

Deleted: c

Deleted: S2

Formatted: English (US)

to a relatively stable interaction process between the strengthened westerly and the EAWM. In addition, the  $^{129}\text{I}$  level in March 625 2018 was much less than that in March 2017, seems to be consequences of weaker EAWM strength in March 2018 compared to in March 2017. This is in good agreement with the EAWM index of 2.04 in 2017 and -1.86 in 2018 (MODES forecast motor

(NCEP I), 2019). The HLP 2 was not the case as HLPs 1 and 3, since the period should be under control of EASM.

The EASM originates from the Pacific and Indian tropical under the role of subtropical highs, and transports moisture from the ocean to East Asia since early summer.  $^{129}\text{I}/^{127}\text{I}$  ratios in the Pacific Ocean, the East China Seas, and the Indian Ocean are as low as  $10^{-10}$  (Liu et al., 2016; Povinec et al., 2011). Even after the Fukushima accident,  $^{129}\text{I}/^{127}\text{I}$  ratios are still less than  $40 \times 10^{-10}$  630 in the western Pacific Ocean (Guilderson et al., 2014). Thus, EASM is poor in  $^{129}\text{I}$  in comparison to the winter monsoon. This is well in agreement with the low  $^{129}\text{I}$  level during the two LLPs (Fig. 2b). The 850 hPa water vapor transmission flow field showed that the southeast wind moisture moving northward to the north of  $35^\circ\text{N}$  May 2, followed by another two 635 outbreaks on May 21 and June 3 (Fig. S5), indicative of EAWM retreat and EASM advance. During this period,  $^{129}\text{I}$  dropped abruptly from  $3.45 \times 10^5$  atoms  $\text{m}^{-3}$  on 27th April to  $1.10 \times 10^5$  atoms  $\text{m}^{-3}$  on 2nd May, followed by a maximum on 8th May, then have a sudden decline to  $0.64 \times 10^5$  atoms  $\text{m}^{-3}$  on 15th May. The violet fluctuation of  $^{129}\text{I}$  is likely caused by the onset of 640 EASM, which is quite violent in a way of stepwise northward jumps. This conclusion is fully supported by the previous metrological observations (Ding and Chan, 2005). As the EASM turned into the active stage since mid-May,  $^{129}\text{I}$  level was low and in a relatively stable state, as showed in the LLP 1.

After the active stage of EASM, however, it is out of the expectation that increased and variable  $^{129}\text{I}$  levels were observed from 645 middle August to early September (HLP 2). The  $^{129}\text{I}$  peak on September 6, 2017 was the highest throughout the sampling year. The back-trajectory model shows that five low-altitude air masses ( $< 1000$  m above ground level) from the Baltic Sea moved fast eastward and arrived at the Guanzhong Basin within five days (Fig. S5e). The Baltic Sea contains high  $^{129}\text{I}$  concentration due to the water exchange with the North Sea that receives over  $100 \text{ kg year}^{-1}$   $^{129}\text{I}$  from La Hague and Sellafield NFRPs (Snyder et al., 2010). Therefore, a  $^{129}\text{I}$  peak observed here indicates the  $^{129}\text{I}$ -enriched westerly has interplayed with the EASM, the latter 650 of which was retreating to the south. It is reported that Xi'an enters into the EASM break stage during this time based on the rainfall data (Ding and Chan, 2005). The intensive interaction between westerly and EASM facilitates the formation of rainfall at their confluence area, resulting in the drastically fluctuating  $^{129}\text{I}$  levels. Therefore, the elevated and variable  $^{129}\text{I}$  levels in HLP 2 can be attributed to the EASM break stage.

After the break stage with significant  $^{129}\text{I}$  fluctuation, the second LLP of  $^{129}\text{I}$  from 21st September to 11th October (LLP 2) 655 occurred when the summer monsoon turns into the revival stage (Fig. 2b). Despite lower than the break period, the  $^{129}\text{I}$  level in this period has slightly increased from  $0.49 \times 10^5$  atoms  $\text{m}^{-3}$  in the active stage to  $0.66 \times 10^5$  atoms  $\text{m}^{-3}$  in the revival stage. After the active-break-revival cycle of summer monsoon reflected by low-high-low  $^{129}\text{I}$  level, the  $^{129}\text{I}$  level has stepwise increased since mid-October, suggesting the EAWM has taken the place of the EASM in the Guanzhong Basin, and last until March next year.

660 To quantitatively characterize the influence of EAM on variation of  $^{129}\text{I}$ , z-normalized  $^{129}\text{I}$  concentrations and  $^{129}\text{I}/^{127}\text{I}$  ratios were used to build a quantitative model during winter monsoon and different stages of the summer monsoon including onset.

**Deleted:** that was weaker than

**Deleted:** was

**Deleted:** the

**Deleted:** S7

**Deleted:** ,

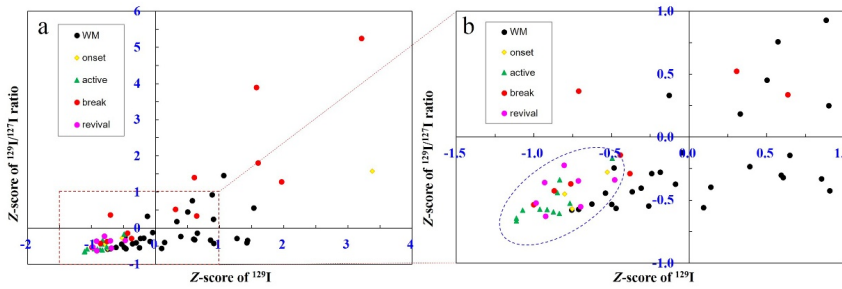
**Deleted:** which

**Deleted:** S5e

**Deleted:** m

**Formatted:** Don't adjust right indent when grid is defined,  
Don't snap to grid

665 active, break, revival and retreat (Fig.6).  $Z(^{129}\text{I})$  varies from -1.11 to 3.38 with a median value of -0.29, and  $Z(^{129}\text{I}/^{127}\text{I}$  ratio) from -0.66 to 5.26 with a median value of -0.34. Based on the observation during 2017/2018 in the Guanzhong Basin, when  $Z(^{129}\text{I})$  is less than -0.5 and  $Z(^{129}\text{I}/^{127}\text{I}$  ratio) is smaller than 0, this period is in good agreement with the onset, active and revival stages of the EASM. During the stable active-stage, z-scores for  $^{129}\text{I}$  and  $^{129}\text{I}/^{127}\text{I}$  were minimal, which was followed by the second lowest value during the revival stage. The onset and break stage showed much larger fluctuation with z-scores changing from -0.8 to -0.3. The break stage of East Asia summer monsoon is an exception, which exists alternative influence from both factors in our studied region. The  $Z(^{129}\text{I})$  from 1.57 to 1.96 of the break stages were even much higher than the period controlled by East Asia winter monsoon with  $Z(^{129}\text{I})$  from -0.5 to 1.53. This result clearly confirms that the EAM plays a decisive role on the temporal variation and long-range transport of not only  $^{129}\text{I}$ , but also other air pollutants (i.e. persisting organic pollutants, inorganic air pollutants) in Chinese monsoon-affected regions.▲



**Deleted:** The influence of EAM on variation of  $^{129}\text{I}$  has been quantitatively characterized using z-score normalized values in supplementary information (SI-4 and Fig.S8), which

**Deleted:** has

**Deleted:** confirms

**Formatted:** Font color: Auto, (Asian) Chinese (China), (Other) English (US)

**Formatted:** Level 2, Space After: 10 pt, Line spacing: single

**Formatted:** Font: 9 pt, Font color: Auto, (Asian) Chinese (China), (Other) English (US)

**Deleted:** Both two iodine isotopes show apparently temporal changes in northwest China, while  $^{129}\text{I}/^{127}\text{I}$  ratios show relatively weak fluctuation (Fig.2c).

**Deleted:** T

**Deleted:** mean

**Formatted:** Not Highlight

**Deleted:**  $101 \pm 124$

**Deleted:** northwest

675

Fig. 6 Two-dimension graph of z-score normalized  $^{129}\text{I}$  concentrations and  $^{129}\text{I}/^{127}\text{I}$  ratios, suggesting the refined features of East Asia summer (onset, active, break and revival in yellow diamond, green triangle, red circle and pink circle, respectively) and winter monsoons (WM, black dot) (a). The coloured symbols clearly demonstrate a detailed cycle of onset-active-break-revival for the summer monsoon with  $Z_{129\text{I}} < 0.5$  and  $Z_{\text{Ratio}} < 0$ , as illustrated in the blue oval area (b).▲

#### 680 4.3 Atmospheric background level of $^{129}\text{I}/^{127}\text{I}$ ratios

**Formatted:** Level 2, Space After: 10 pt, Line spacing: single

For the purpose of nuclear environment safety monitoring, the average  $^{129}\text{I}/^{127}\text{I}$  ratio of  $(92.7 \pm 124) \times 10^{-10}$  can be simply regarded as the atmospheric background level of  $^{129}\text{I}$  in northwest China. The previous studies on  $^{129}\text{I}$  environmental baseline have never carefully investigate the influence of climate on time variation of  $^{129}\text{I}$ . Here our day-resolution  $^{129}\text{I}$  dataset in this monsoon climate city showed that time variation of the atmospheric baseline level related to metrological conditions, heavy haze events and atmospheric circulation, has to be carefully considered and used for better evaluation of the impact of possible nuclear incidents in a practical way. Particularly, a pilot nuclear reprocessing plants locating upwind to Xi'an, might be extended and will be a source of radionuclides in the future. The baseline established in this work is, therefore, of significance to long-term monitor nuclear environmental safety, and to sensitively assess the impact of nuclear incidents and apply on environmental process tracing.

**Formatted:** Font color: Auto, (Asian) Chinese (China), (Other) English (US)

**Deleted:** Both two iodine isotopes show apparently temporal changes in northwest China, while  $^{129}\text{I}/^{127}\text{I}$  ratios show relatively weak fluctuation (Fig.2c).

**Deleted:** T

**Deleted:** mean

**Formatted:** Not Highlight

**Deleted:**  $101 \pm 124$

**Deleted:** northwest

## 5 Conclusions

The study firstly presents a high-resolution temporal variation of atmospheric  $^{127}\text{I}$  and  $^{129}\text{I}$  in northwest China, showing the vivid seasonal characteristics of iodine isotopes and an  $^{129}\text{I}/^{127}\text{I}$  baseline ratio of  $(92.7 \pm 124) \times 10^{-10}$ . Variation of  $^{127}\text{I}$  strongly linking with atmospheric pollutions and heavy haze episodes, in particular in winter, indicates that  $^{127}\text{I}$  in Xi'an aerosols mainly derives from combustion of fossil fuel. Aerosol  $^{129}\text{I}$  mainly originates from European nuclear reprocessing plants through long-range transport, and its temporal variation is strongly dominated by the interplay of East Asian winter and summer monsoon. Previous studies on temporal changes of atmospheric  $^{129}\text{I}$  in other monsoonal regions showed a simple pattern with lowest level in summer and highest in winter, while our day-resolution dataset showed that high  $^{129}\text{I}$  levels could be found in summer time due to the break of East Asian summer monsoon. The locally input  $^{127}\text{I}$  and exogenous  $^{129}\text{I}$  were greatly increased during haze events, reflecting the possible role of iodine in the formation of urban fine particles, therefore, further investigations are expected to focus on the speciation of iodine isotopes for mechanism study of iodine's impact on air pollution.

**Formatted:** Not Highlight

**Deleted:**  $101 \pm 129$

## Supplement

Supplementary information accompanies this paper in a separate file.

## 715 Author contribution

LZ, XH and SX designed and optimized the experiment. LZ, and NC performed the experiment, with the help of PC and YF. TF collected the air pollutant data. LZ, TF, PC, and YF draw the figures. The data analysis and interpretation were carried out by LZ, XH, SX, TF and NC. LZ prepared the paper, with contributions from all co-authors.

## Competing interests

720 The authors declare that they have no conflict of interests.

## Acknowledgement

This work was supported by the National Natural Science Foundation of China (No. 11605207 and 41603125), the Youth Innovation Promotion Association of CAS, the Ministry of Science and Technology basic project (No. 2015FY110800), the Bureau of International Co-operation, CAS (132B61KYSB20180003) and National Research Program for Key Issues in Air

725 Pollution Control (DQGG0105). L.Z. also gratefully acknowledges Dr. Q. Liu, Ms. M. Fang, [Ms. Y. Wang](#), Mr. L. Wang and Mr. J. Zhou in IEECAS for their kind help on AMS measurement, sample collection and figure drawing. [We acknowledge the two anonymous referees for their constructive comments.](#)

**Deleted:** -02

## References

An, Z., Colman, S. M., Zhou, W., Li, X., Brown, E. T., Jull, A. J. T., Cai, Y., Huang, Y., Lu, X., Chang, H., Song, Y., Sun, Y., Xu, H., Liu, W., Jin, Z., Liu, X., Cheng, P., Liu, Y., Ai, L., Li, X., Liu, X., Yan, L., Shi, Z., Wang, X., Wu, F., Qiang, X., Dong, J., Lu, F. and Xu, X.: Interplay between the Westerlies and Asian monsoon recorded in Lake Qinghai sediments since 32 ka, *Sci. Rep.*, 2, 619 [online] Available from: <https://doi.org/10.1038/srep00619>, 2012.

735 Ayers, G. P., Penkett, S. A., Gillett, R. W., Bandy, B., Galbally, I. E., Meyer, C. P., Elsworth, C. M., Bentley, S. T. and Forgan, B. W.: The annual cycle of peroxides and ozone in marine air at Cape Grim, Tasmania, *J. Atmos. Chem.*, 23(3), 221–252, doi:10.1007/BF00055155, 1996.

Brauer, F. P., Rieck, H. G. J. and Hooper, R. L.: Particulate and gaseous atmospheric iodine concentrations, IAEA, International Atomic Energy Agency (IAEA), 1973.

740 Carpenter, L. J., MacDonald, S. M., Shaw, M. D., Kumar, R., Saunders, R. W., Parthipan, R., Wilson, J. and Plane, J. M. C.: Atmospheric iodine levels influenced by sea surface emissions of inorganic iodine, *Nat. Geosci.*, 6(2), 108–111, doi:10.1038/ngeo1687, 2013.

Cheng, N., Duan, L., Xiu, G., Zhao, M. and Qian, G.: Comparison of atmospheric PM2.5-bounded mercury species and their correlation with bromine and iodine at coastal urban and island sites in the eastern China, *Atmos. Res.*, 183, 17–25, 745 doi:10.1016/j.atmosres.2016.08.009, 2017.

China Meteororological Administration: Sandstorm in northwest China and central and western Inner Mongolia, Webpage [online] Available from: [http://www.cma.gov.cn/2011xwzx/2011xqxxw/2011xzytq/201704/t20170417\\_407699.html](http://www.cma.gov.cn/2011xwzx/2011xqxxw/2011xzytq/201704/t20170417_407699.html) (Accessed 10 October 2018), 2017.

Cohen, B. L.: The origin of I in soil and the  $^{129}\text{I}$  problem, *Health Phys.*, 49(2), 279–285, 1985.

750 Ding, Y. and Chan, J. C. L.: The East Asian summer monsoon: An overview, *Meteorol. Atmos. Phys.*, 89(1–4), 117–142, doi:10.1007/s00703-005-0125-z, 2005.

Dong, Z., Shao, Y., Qin, D., Zhang, L., Hou, X., Wei, T., Kang, S. and Qin, X.: Insight Into Radio-Isotope  $^{129}\text{I}$  Deposition in Fresh Snow at a Remote Glacier Basin of Northeast Tibetan Plateau, China, *Geophys. Res. Lett.*, 0(0), doi:10.1029/2018GL078480, 2018.

755 Duan, D.: Concentration Characteristics of Atmospheric Particulate Matters and Iodine in Coal-fired Area, Nanchang University., 2018.

Englund, E., Aldahan, A., Hou, X., Possnert, G. and Soderstrom, C.: Iodine (I-129 and I-127) in aerosols from northern Europe, *Nucl.Instrum.Meth.B*, 268(7–8), 1139–1141, 2010.

Fan, Y.: Spatial distribution of  $^{129}\text{I}$  in Chinese surface soil and preliminary study on the  $^{129}\text{I}$  chronology, PhD thesis. Inst. Earth Environ. Chinese Acad. Sci., 2013.

760 Fan, Y., Hou, X., Zhou, W. and Liu, G.: I record of nuclear activities in marine sediment core from Jiaozhou Bay in China, *J. Environ. Radioact.*, 154(March 2011), 15–24, doi:10.1016/j.jenvrad.2016.01.008, 2016.

Fehn, U., Moran, J. E., Snyder, G. T. and Muramatsu, Y.: The initial  $^{129}\text{I}/\text{I}$  ratio and the presence of “old” iodine in continental margins, *Nucl.Instrum.Meth.B*, 259(1), 496–502, 2005.

**Formatted:** Superscript

**Formatted:** Superscript

**Formatted:** Superscript

**Formatted:** Superscript

**Formatted:** Superscript

765 Fuge, R. and Johnson, C.: The geochemistry of iodine - a review, Environ. Geochem. Health, 8(2), 31–54, doi:10.1007/BF02311063, 1986.

Gao, Y., Sun, M., Wu, X., Liu, Y., Guo, Y. and Wu, J.: Concentration characteristics of bromine and iodine in aerosols in Shanghai, China, Atmos. Environ., 44, 4298–4302, doi:10.1016/j.atmosenv.2010.05.047, 2010.

770 Guilderson, T. P., Tumey, S. J., Brown, T. a. and Buesseler, K. O.: The 129-iodine content of subtropical Pacific waters: impact of Fukushima and other anthropogenic  $^{129}\text{I}$  sources, Biogeosciences, 11, 4839–4852, doi:10.5194/bg-10-19935-2013, 2014.

**Formatted:** Superscript

Hasegawa, H., Kakiuchi, H., Akata, N., Ohtsuka, Y. and Hisamatsu, S.: Regional and global contributions of anthropogenic iodine-129 in monthly deposition samples collected in North East Japan between 2006 and 2015, J. Environ. Radioact., 171, 65–73, doi:10.1016/J.JENVRAD.2017.01.027, 2017.

775 He, C., Hou, X., Zhao, Y., Wang, Z., Li, H., Chen, N., Liu, Q., Zhang, L., Luo, M., Liang, W., Fan, Y. and Zhao, X. L.:  $^{129}\text{I}$  level in seawater near a nuclear power plant determined by accelerator mass spectrometer, Nucl. Instruments Methods Phys. Res. Sect. A, 632(1), 152–156, doi:10.1016/j.nima.2010.12.182, 2011.

**Formatted:** Superscript

He, L.: Iodine concentration, chemical speciation and their distribution in atmospheric precipitation and soil, Nanchang University, China., 2012.

780 Hou, X., Aldahan, A., Nielsen, S. P., Possnert, G., Hou, X., Aldahan, A., Nielsen, S. P. and Possnert, G.: Time Series of I-129 and I-127 Speciation in Precipitation from Denmark, Environ. Sci. Technol., 43(17), 6522–6528, doi:10.1021/es9012678, 2009.

Jabbar, T., Wallner, G. and Steier, P.: A review on  $^{129}\text{I}$  analysis in air, J. Environ. Radioact., 126, 45–54, 2013.

**Formatted:** Superscript

Jackson, D., Ibrahim, F., Fulker, M. J., Parry, S. J. and Rackham, K.: The effect of chemical speciation on the impact of I 785 discharges to atmosphere from BNFL Sellafield, Cumbria, Radioprotection, 37(C1), 459–464, 2002.

Kadowaki, M., Katata, G., Terada, H., Suzuki, T., Hasegawa, H., Akata, N. and Kakiuchi, H.: Impacts of anthropogenic source from the nuclear fuel reprocessing plants on global atmospheric iodine-129 cycle: A model analysis, Atmos. Environ., 184(April), 278–291, doi:10.1016/j.atmosenv.2018.04.044, 2018.

Küpper, F. C., Carpenter, L. J., McFiggans, G. B., Palmer, C. J., Waite, T. J., Boneberg, E.-M., Woitsch, S., Weiller, M., 790 Abela, R., Grolimund, D., Potin, P., Butler, A., Luther, G. W. 3rd, Kroneck, P. M. H., Meyer-Klaucke, W. and Feiters, M. C.: Iodide accumulation provides kelp with an inorganic antioxidant impacting atmospheric chemistry, Proc. Natl. Acad. Sci., 105(19), 6954–6958, 2008.

Liu, D., Hou, X., Du, J., Zhang, L. and Zhou, W.:  $^{129}\text{I}$  and its species in the East China Sea: level, distribution, sources and tracing water masses exchange and movement, Sci. Rep., 6(October), 36611, doi:10.1038/srep36611, 2016.

**Formatted:** Superscript

795 McFiggans, G., Plane, J. M. C., Allan, B. J., Carpenter, L. J., Coe, H. and O'Dowd, C.: A modeling study of iodine chemistry in the marine boundary layer, J. Geophys. Res. Atmos., 105(D11), 14371–14385, doi:10.1029/1999JD901187, 2000.

Michel, R., Daraoui, A., Gorny, M., Jakob, D., Sachse, R., Tosch, L., Nies, H., Goroncy, I., Herrmann, J., Synal, H. A., Stocker, M. and Alfimov, V.: Iodine-129 and iodine-127 in European seawaters and in precipitation from Northern Germany, Sci.Total

Environ., 419, 151–169, 2012.

800 Ministry of Environmental Protection of the People's Republic of China: Environmental radiation monitoring results of the sixth North Korean nuclear test in the northeast border and surrounding areas., 2017.

MODES forecast motor (NCEP I): East Asian Winter Monsoon Index, Beijing Clim. Cent. [online] Available from: [https://cmdp.ncc-cma.net/pred/cn\\_peace.php?eYear=2017&eMonth=5&search=e%D0%CE\\_2'&product=EAWM.MODES#search](https://cmdp.ncc-cma.net/pred/cn_peace.php?eYear=2017&eMonth=5&search=e%D0%CE_2'&product=EAWM.MODES#search) (Accessed 8 July 2019), 2019.

Moran, J. E., Oktay, S. D., Santschi, P. H. and Schink, D. R.: Atmospheric dispersal of iodine-129 from nuclear fuel reprocessing facilities, Environ. Sci. Technol., 33(15), 2536–2542, 1999.

Povinec, P. P., Breier, R., Coppola, L., Groening, M., Jeandel, C., Jull, A. J. T., Kieser, W. E., Lee, S. H., Lioung, W. K., Morgenstern, U., Park, Y. H. and Top, Z.: Tracing of water masses using a multi isotope approach in the southern Indian 810 Ocean, Earth Planet. Sci. Lett., 302(1–2), 14–26, 2011.

Saiz-Lopez, A., Gómez Martin, J. C., Plane, J. M. C., Saunders, R. W., Baker, A. R., Von Glasow, R., Carpenter, L. J. and McFiggans, G.: Atmospheric chemistry of iodine, Chem. Rev., 112(3), 1773–1804, 2012.

Santos, F. J., López-Gutiérrez, J. M., García-León, M., Suter, M. and Synal, H. A.: Determination of  $^{129}\text{I}/^{127}\text{I}$  in aerosol samples in Seville (Spain), J. Environ. Radioact., 84(1), 103–109, 2005.

815 Shaanxi Provincial Bureau of Statistics: Report of industrial coal reduction in Guanzhong Basin in 2017, Xi'an, China. [online] Available from: <http://www.shaanxitj.gov.cn/site/1/html/126/131/138/17703.htm>, 2018.

Sive, B. C., Varner, R. K., Mao, H., Talbot, R., Blake, D. R. and Wingenter, O. W.: A large terrestrial source of methyl iodide, Geophys. Res. Lett., 34(17), 2007.

Snyder, G., Aldahan, A., Aldahan, A. and Possnert, G.: Global distribution and long-term fate of anthropogenic  $^{129}\text{I}$  in marine 820 and surface water reservoirs, Geochemistry, Geophys. Geosystems, 11(4), 1–19, 2010.

Toyama, C., Muramatsu, Y., Igarashi, Y., Aoyama, M. and Matsuzaki, H.: Atmospheric fallout of  $^{129}\text{I}$  in Japan before the Fukushima accident: Regional and global contributions (1963–2005), Environ. Sci. Technol., 47(15), 8383–8390, doi:10.1021/es401596z, 2013.

Tsukada, H., Ishida, J. and Narita, O.: Particle-size distributions of atmospheric  $^{129}\text{I}$  and  $^{127}\text{I}$  aerosols, Atmos. Environ. Part A, 825 25(5–6), 905–908, doi:[http://dx.doi.org/10.1016/0960-1686\(91\)90132-Q](http://dx.doi.org/10.1016/0960-1686(91)90132-Q), 1991.

Wershofen, H. and Aumann, D. C.: Iodine-129 in the environment of a nuclear fuel reprocessing plant: VII. Concentrations and chemical forms of  $^{129}\text{I}$  and  $^{127}\text{I}$  in the atmosphere, J. Environ. Radioact., 10(2), 141–156, 1989.

Whitehead, D. C.: The distribution and transformations of iodine in the environment, Environ. Int., 10(4), 321–339, doi:10.1016/0160-4120(84)90139-9, 1984.

830 World Nuclear Association: <http://www.world-nuclear.org/>, Last access 9 Jan 2017, 2017.

Wu, D., Du, J., Deng, H., Wang, W., Xiao, H. and Li, P.: Estimation of atmospheric iodine emission from coal combustion, Int. J. Environ. Sci. Technol., 11(2), 357–366, doi:10.1007/s13762-013-0193-4, 2014.

Xi'an Bureau of Statistics: Xi'an Statistics Yearbook. [online] Available from: <http://tjj.xa.gov.cn/ptl/def/def/2017/zk/indexch.htm>, 2018.

835 Xu, S., Xie, Z., Li, B., Liu, W., Sun, L., Kang, H., Yang, H. and Zhang, P.: Iodine speciation in marine aerosols along a 15000-km round-trip cruise path from Shanghai, China, to the Arctic Ocean, *Environ. Chem.*, 7(5), 406–412 [online] Available from: <http://dx.doi.org/10.1071/EN10048>, 2010.

Xu, S., Freeman, S. P. H. T. S. P. H. T., Hou, X., Watanabe, A., Yamaguchi, K. and Zhang, L.: Iodine Isotopes in Precipitation: Temporal Responses to  $^{129}\text{I}$  Emissions from the Fukushima Nuclear Accident, *Environ. Sci. Technol.*, 47(19), 10851–10859, 840 doi:10.1021/es401527q, 2013.

Xu, S., Zhang, L., Freeman, S. P. H. T., Hou, X., Shibata, Y., Sanderson, D., Cresswell, A., Doi, T. and Tanaka, A.: Speciation of Radiocesium and Radioiodine in Aerosols from Tsukuba after the Fukushima Nuclear Accident, *Environ. Sci. Technol.*, 49(2), 1017–1024, doi:10.1021/es504431w, 2015.

Zhang, L., Zhou, W. J., Hou, X., Chen, N., Liu, Q., He, C., Fan, Y., Luo, M., Wang, Z. and Fu, Y.: Level and source of  $^{129}\text{I}$  of 845 environmental samples in Xi'an region, China, *Sci. Total Environ.*, 409(19), 3780–3788, doi:10.1016/j.scitotenv.2011.06.007, 2011a.

Zhang, L., Hou, X. and Xu, S.: Speciation of  $^{127}\text{I}$  and  $^{129}\text{I}$  in atmospheric aerosols at Riso, Denmark: Insight into sources of iodine isotopes and their species transformations, *Atmos. Chem. Phys.*, 16, 1971–1985, 2016.

Zhang, L., Hou, X., Li, H. and Xu, X.: A 60-year record of  $^{129}\text{I}$  in Taal Lake sediments (Philippines): Influence of human 850 nuclear activities at low latitude region, *Chemosphere*, 193, 1149–1156, doi:10.1016/j.chemosphere.2017.11.134, 2018a.

Zhang, L., Hou, X., Fu, Y., Fang, M. and Chen, N.: Determination of  $^{129}\text{I}$  in aerosols using pyrolysis and AgI–AgCl coprecipitation separation and accelerator mass spectrometry measurements, *J. Anal. At. Spectrom.*, 33, 1729–1736, doi:10.1039/C8JA00248G, 2018b.

**Formatted:** Superscript

**Formatted:** Superscript

**Deleted:** Zhang, L., Zhou, W. J., Hou, X., Chen, N., Liu, Q., He, C., Fan, Y., Luo, M., Wang, Z. and Fu, Y.: Level and source of I-129 of environmental samples in Xi'an region, China, *Sci. Total Environ.*, 409(19), 3780–3788, doi:10.1016/j.scitotenv.2011.06.007, 2011b.

**Formatted:** Superscript

**Formatted:** Superscript

**Formatted:** Superscript

**Formatted:** Superscript

**Page 3: [1] Deleted** Luyuan Zhang **12/12/19 5:11:00 PM**

▼  
▲ **Page 8: [2] Deleted** Luyuan Zhang **12/18/19 10:18:00 AM**

▼  
▲ **Page 8: [2] Deleted** Luyuan Zhang **12/18/19 10:18:00 AM**

▼  
▲ **Page 8: [3] Deleted** Luyuan Zhang **12/18/19 10:18:00 AM**

▼  
▲ **Page 8: [3] Deleted** Luyuan Zhang **12/18/19 10:18:00 AM**

▼  
▲ **Page 8: [3] Deleted** Luyuan Zhang **12/18/19 10:18:00 AM**

▼  
▲ **Page 8: [4] Deleted** Luyuan Zhang **1/7/20 1:47:00 PM**

▼  
▲ **Page 8: [4] Deleted** Luyuan Zhang **1/7/20 1:47:00 PM**

▼  
▲ **Page 8: [4] Deleted** Luyuan Zhang **1/7/20 1:47:00 PM**

▼  
▲ **Page 8: [5] Deleted** Luyuan Zhang **1/7/20 1:48:00 PM**

▼  
▲ **Page 8: [5] Deleted** Luyuan Zhang **1/7/20 1:48:00 PM**

▼  
▲ **Page 8: [6] Deleted** Luyuan Zhang **12/18/19 11:39:00 AM**

▼  
▲ **Page 8: [6] Deleted** Luyuan Zhang **12/18/19 11:39:00 AM**

▼  
▲ **Page 8: [6] Deleted** Luyuan Zhang **12/18/19 11:39:00 AM**

▼  
▲ **Page 8: [6] Deleted** Luyuan Zhang **12/18/19 11:39:00 AM**

▼  
▲ **Page 8: [6] Deleted** Luyuan Zhang **12/18/19 11:39:00 AM**

**Page 8: [6] Deleted** Luyuan Zhang 12/18/19 11:39:00 AM

▼

▲

**Page 8: [6] Deleted** Luyuan Zhang 12/18/19 11:39:00 AM

▼

▲

**Page 8: [6] Deleted** Luyuan Zhang 12/18/19 11:39:00 AM

▼

▲

**Page 8: [6] Deleted** Luyuan Zhang 12/18/19 11:39:00 AM

▼

▲

**Page 8: [7] Formatted** Luyuan Zhang 12/16/19 4:00:00 PM

Font: (Default) Times New Roman

▲

**Page 8: [7] Formatted** Luyuan Zhang 12/16/19 4:00:00 PM

Font: (Default) Times New Roman

▲

**Page 8: [8] Deleted** Luyuan Zhang 12/16/19 2:24:00 PM

▼

▲

**Page 8: [8] Deleted** Luyuan Zhang 12/16/19 2:24:00 PM

▼

▲

**Page 8: [8] Deleted** Luyuan Zhang 12/16/19 2:24:00 PM

▼

▲

**Page 8: [8] Deleted** Luyuan Zhang 12/16/19 2:24:00 PM

▼

▲

**Page 8: [8] Deleted** Luyuan Zhang 12/16/19 2:24:00 PM

▼

▲

**Page 8: [8] Deleted** Luyuan Zhang 12/16/19 2:24:00 PM

▼

▲

**Page 8: [9] Deleted** Luyuan Zhang 12/16/19 8:27:00 AM

▼

▲

**Page 8: [9] Deleted** Luyuan Zhang 12/16/19 8:27:00 AM

▼

▲

**Page 8: [9] Deleted** Luyuan Zhang 12/16/19 8:27:00 AM

▼

▲

**Page 8: [9] Deleted** Luyuan Zhang 12/16/19 8:27:00 AM

**Page 8: [9] Deleted** Luyuan Zhang **12/16/19 8:27:00 AM**

▼  
▲ **Page 8: [9] Deleted** Luyuan Zhang **12/16/19 8:27:00 AM**

▼  
▲ **Page 8: [9] Deleted** Luyuan Zhang **12/16/19 8:27:00 AM**

▼  
▲ **Page 8: [10] Formatted** Luyuan Zhang **1/9/20 11:10:00 AM**

Font: (Default) Times New Roman

▲ **Page 8: [10] Formatted** Luyuan Zhang **1/9/20 11:10:00 AM**

Font: (Default) Times New Roman

▲ **Page 13: [11] Deleted** Luyuan Zhang **12/16/19 6:28:00 PM**

▼  
▲ **Page 13: [11] Deleted** Luyuan Zhang **12/16/19 6:28:00 PM**

▼  
▲ **Page 13: [12] Formatted** Luyuan Zhang **1/7/20 3:20:00 PM**

Font color: Text 1

▲ **Page 13: [12] Formatted** Luyuan Zhang **1/7/20 3:20:00 PM**

Font color: Text 1

▲ **Page 13: [12] Formatted** Luyuan Zhang **1/7/20 3:20:00 PM**

Font color: Text 1

▲ **Page 13: [13] Formatted** Luyuan Zhang **1/7/20 3:20:00 PM**

Font color: Text 1

▲ **Page 13: [13] Formatted** Luyuan Zhang **1/7/20 3:20:00 PM**

Font color: Text 1

▲ **Page 13: [13] Formatted** Luyuan Zhang **1/7/20 3:20:00 PM**

Font color: Text 1

▲ **Page 13: [14] Deleted** Luyuan Zhang **1/7/20 2:09:00 PM**

▼  
▲ **Page 13: [14] Deleted** Luyuan Zhang **1/7/20 2:09:00 PM**

▼  
▲ **Page 13: [15] Deleted** Luyuan Zhang **1/7/20 2:11:00 PM**

**Page 13: [15] Deleted** Luyuan Zhang **1/7/20 2:11:00 PM**

▼  
▲ **Page 13: [15] Deleted** Luyuan Zhang **1/7/20 2:11:00 PM**

▼  
▲ **Page 13: [16] Deleted** Luyuan Zhang **12/20/19 4:08:00 PM**

▼  
▲ **Page 13: [16] Deleted** Luyuan Zhang **12/20/19 4:08:00 PM**

▼  
▲ **Page 13: [17] Deleted** Luyuan Zhang **12/19/19 5:15:00 PM**

▼  
▲ **Page 13: [17] Deleted** Luyuan Zhang **12/19/19 5:15:00 PM**

▼  
▲ **Page 13: [18] Deleted** Luyuan Zhang **12/18/19 4:41:00 PM**

▲ **Page 13: [19] Formatted** Luyuan Zhang **12/18/19 4:30:00 PM**

Font: 7 pt

▲ **Page 13: [19] Formatted** Luyuan Zhang **12/18/19 4:30:00 PM**

Font: 7 pt

▲ **Page 13: [19] Formatted** Luyuan Zhang **12/18/19 4:30:00 PM**

Font: 7 pt

▲ **Page 13: [19] Formatted** Luyuan Zhang **12/18/19 4:30:00 PM**

Font: 7 pt

▲ **Page 13: [19] Formatted** Luyuan Zhang **12/18/19 4:30:00 PM**

Font: 7 pt

▲ **Page 13: [19] Formatted** Luyuan Zhang **12/18/19 4:30:00 PM**

Font: 7 pt

▲ **Page 13: [19] Formatted** Luyuan Zhang **12/18/19 4:30:00 PM**

Font: 7 pt

▲ **Page 13: [19] Formatted** Luyuan Zhang **12/18/19 4:30:00 PM**

Font: 7 pt

▲ **Page 13: [19] Formatted** Luyuan Zhang **12/18/19 4:30:00 PM**

Font: 7 pt

Font: 7 pt

▲ **Page 13: [19] Formatted**

**Luyuan Zhang**

**12/18/19 4:30:00 PM**

Font: 7 pt

▲ **Page 13: [19] Formatted**

**Luyuan Zhang**

**12/18/19 4:30:00 PM**

Font: 7 pt

▲ **Page 13: [19] Formatted**

**Luyuan Zhang**

**12/18/19 4:30:00 PM**

Font: 7 pt

▲ **Page 13: [19] Formatted**

**Luyuan Zhang**

**12/18/19 4:30:00 PM**

Font: 7 pt

▲ **Page 13: [19] Formatted**

**Luyuan Zhang**

**12/18/19 4:30:00 PM**

Font: 7 pt

▲ **Page 13: [19] Formatted**

**Luyuan Zhang**

**12/18/19 4:30:00 PM**

Font: 7 pt

▲ **Page 13: [19] Formatted**

**Luyuan Zhang**

**12/18/19 4:30:00 PM**

# Temporal variation of $^{129}\text{I}$ and $^{127}\text{I}$ in aerosols from Xi'an, China: influence of East Asian monsoon and heavy haze events

Luyuan Zhang <sup>1,2,3,5\*</sup>, Xiaolin Hou <sup>1,2,3,5</sup>, Sheng Xu <sup>4</sup>, Tian Feng <sup>1</sup>, Peng Cheng <sup>1</sup>, Yunchong Fu <sup>1</sup>, Ning Chen <sup>1</sup>

<sup>5</sup> State Key Laboratory of Loess and Quaternary Geology, Shaanxi Key Laboratory of Accelerator Mass Spectrometry Technology and Application, Xi'an AMS Center, Institute of Earth Environment CAS, Xi'an 710061, China

<sup>2</sup>Center for Excellence in Quaternary Science and Global Change, Chinese Academy of Sciences, Xian 710061, China

<sup>3</sup>Center for Nuclear Technologies, Technical University of Denmark, Risø Campus, Roskilde 4000, Denmark

<sup>4</sup>Institute of Surface-Earth System Science, Tianjin University, Tianjin 300072, China

<sup>10</sup>Open Studio for Oceanic-Continental Climate and Environment Changes, Pilot National Laboratory for Marine Science and Technology (Qingdao), Qingdao 266061, China

Correspondence to: Luyuan Zhang (zhangluyuan.118@163.com)

The supplementary information includes ~~five~~ figures and ~~one~~ table.

## 15 SI-1 Determination of $^{129}\text{I}$ and $^{127}\text{I}$ in aerosol samples

### SI-1.1 Aerosol sampling

The aerosol samples were collected by a high-volume sampler onto glass fibre filters (200 mm×250 mm, Tianhong Instrument Ltd., Wuhan, China). The flow rate is  $1.5 \text{ m}^3 \text{ min}^{-1}$  and the sample duration was 24 h for each filter with air flux of  $2100 \text{ m}^3$ .

The sampler is installed on the roof of the Xi'an AMS Centre in Xi'an, China ( $34^{\circ}13'25''\text{N}$ ,  $109^{\circ}0'0''\text{E}$ ) with an elevation of

20 440 m above mean sea level (Fig.1).

### SI-1.2. Iodine isotopes analysis

68 aerosol filters, about four filter samples in each month, were selected for measurement of iodine isotopes. Each filter represents one day information. Half of one filter with air flux of about  $1000 \text{ m}^3$  was analysed for ~~iodine isotopes~~, and the other half was reserved for other ~~purpose~~. Iodine was separated from the aerosol filter using pyrolysis and  $\text{AgI-AgCl}$

25 coprecipitation in combination with accelerator mass spectrometry (AMS) for measurement, as described elsewhere (Zhang et al., 2018b). In brief, the aerosol samples were placed into a corundum boat.  $^{125}\text{I}$  in the form of iodide was added for calculation of chemical yield. Iodine in the samples was released as gaseous form at high temperature in the atmosphere of nitrogen and oxygen gases in a tube furnace (Hou et al., 2010). The released iodine was trapped into a solution containing  $0.5 \text{ mol L}^{-1}$   $\text{NaOH}$  and  $0.02 \text{ mol L}^{-1}$   $\text{NaHSO}_3$ . An aliquot of solution (1.0 mL) was taken for determination of  $^{127}\text{I}$  using ICP-MS (Agilent 8800, USA). Another 1.0 mL solution was taken to a tube and counted for  $^{125}\text{I}$  using a NaI gamma counter (Model FJ2021, Xi'an

**Deleted:** <sup>1</sup>

**Formatted:** English (UK)

**Formatted:** English (US)

**Deleted:** seven

**Deleted:** two

**Deleted:** s

**Deleted:** Xi'an, located in the Guanzhong basin, is the largest city in northwest China with a population of 9.9 million. The basin is nestled between the Qin Ling in the south and the Loess Plateau in the north, and is warm temperate zone with semihumid continental monsoon climate (Fig.1b).

**Deleted:** 129I

**Formatted:** Not Superscript/ Subscript

**Formatted:** Not Superscript/ Subscript

**Deleted:** use

Nuclear Instrument Factory, China) to calculate the chemical yield of iodine during combustion. After gamma measurement, 0.2 mg  $^{127}\text{I}$  carrier (Woodward Company, USA) was added to the trap solution. For procedure blank samples, 0.2 mg iodine and 0.5 mg chloride (as NaCl) was added. 1 mL of 0.5 M NaHSO<sub>3</sub> was used to reduce iodate to iodide. The solution was firstly

45 adjusted to pH < 2 by 3 M HNO<sub>3</sub>, then 1 mL 0.5 M AgNO<sub>3</sub> solution was added to the solution to precipitate iodine as AgI-AgCl coprecipitation. The formed AgI-AgCl precipitate was washed once with 3 M HNO<sub>3</sub> to remove Ag<sub>2</sub>SO<sub>3</sub> and Ag<sub>2</sub>SO<sub>4</sub>, then washed with deionized water once and 5-20% ammonium hydroxide once to remove excessive AgCl, and finally rinsed twice with deionized water. After centrifugation, the AgI-AgCl coprecipitate was ready for AMS measurement. The procedural blank was prepared using a blank glass fibre filter with the same procedure as that for samples.

#### 50 SI-1.3 AMS and ICP-MS determination of $^{129}\text{I}$ and $^{127}\text{I}$

The prepared AgI-AgCl coprecipitates were completely dried at 70°C, then mixed with Nb metal powder (99.9%, 325 mesh, Alfa Aesar, USA) in a mass ratio of 1:5 and pressed into copper target holders.  $^{129}\text{I}$  in the target was measured using a 3MV AMS in the Xi'an AMS Centre (Hou et al., 2010). A voltage of 2.5 MV was applied for measurement of  $^{129}\text{I}/^{127}\text{I}$  atomic ratios. +5 charge state of iodine ion was selected and extracted from the accelerator by a magnetic analyser.  $^{129}\text{I}/^{127}\text{I}$  ratios of the iodine carrier are determined to be less than  $2 \times 10^{-13}$ . The analytical precision was less than 5% for all the samples.

55 The trapping solution was diluted by a factor of 20-50 with 1% NH<sub>3</sub>·H<sub>2</sub>O, and analysed for  $^{127}\text{I}$  concentration by ICP-MS (Agilent 8800, USA) using the mode of single quadrupole and no dynamic collision-reaction gas. Cs<sup>+</sup> (CsCl) was used as an internal standard in the ICP-MS measurement of iodine. The sensitivity of  $^{127}\text{I}$  is 250 Mcps per 1 mg L<sup>-1</sup> of iodine, and the instrumental detection limit is 0.002  $\mu\text{g L}^{-1}$  for  $^{127}\text{I}$ .

#### 60 SI-1.4 Calculation of z-score of $^{129}\text{I}$ concentrations and $^{129}\text{I}/^{127}\text{I}$ ratios

Z-scores of  $^{129}\text{I}$  concentrations and  $^{129}\text{I}/^{127}\text{I}$  ratios are calculated by subtracting the sample mean from an individual raw score and then dividing the difference by the sample standard deviation (Eq.1). The absolute value of z-score represents the distance between the raw  $^{129}\text{I}$  concentrations and  $^{129}\text{I}/^{127}\text{I}$  ratios and the sample mean in units of the standard deviation.

$$z = \frac{x-\bar{x}}{s} \quad \text{Eq. (1)}$$

65 Where,  $\bar{x}$  is the mean of the sample;  $S$  is the standard deviation of the sample;  $z$  is negative when the raw score is below the mean, positive when above.

#### SI-2. Influence of precipitation and wind speed

Precipitation. Wet and dry deposition are vital pathways of iodine removal from the atmosphere. The effect of rainfall on iodine concentrations in aerosols is not clear. Xi'an is a warm temperate semihumid continental monsoon climate, with annual 70 precipitation of 522.4-719.5 mm. The annual precipitation was 649.0 mm in 2017, and precipitations in September and October

**Deleted:** .

**Deleted:** directly

**Deleted:** sample

**Deleted:** bronze

**Deleted:** i

**Deleted:** The

**Deleted:** is

**Formatted:** English (US)

#### Deleted: SI-2 Monthly and seasonal variations

$^{127}\text{I}$  and  $^{129}\text{I}$  in aerosols are characterized with the apparent monthly and seasonal variations (Fig.S1 and S2). The minimum and maximum of monthly concentrations were observed in August and December for  $^{127}\text{I}$ , and July and December for  $^{129}\text{I}$ , respectively.  $^{127}\text{I}$  concentrations in November, December and January (11.4-12.7  $\mu\text{g m}^{-3}$ ) were more than two times higher than those in other months (3.12-6.70  $\mu\text{g m}^{-3}$ ). Distinct from  $^{127}\text{I}$ , monthly variation of  $^{129}\text{I}$  shows the lowest level in June and July ((0.47-0.50)  $\times 10^5$  atoms m<sup>-3</sup>), about two to six times lower than other months. The maximum of  $^{129}\text{I}/^{127}\text{I}$  ratio was not observed in winter months but in September. The mean  $^{127}\text{I}$  concentrations were 5.68±2.34  $\mu\text{g m}^{-3}$ , 3.61±1.49  $\mu\text{g m}^{-3}$ , 6.05±4.52  $\mu\text{g m}^{-3}$ , and 10.6±6.0  $\mu\text{g m}^{-3}$  in spring, summer, fall and winter, respectively. The level of  $^{127}\text{I}$  in winter was about two times higher than spring and fall, three times higher than summer.  $^{129}\text{I}$  were (2.10±1.83)  $\times 10^5$  atoms m<sup>-3</sup>, (1.24±1.54)  $\times 10^5$  atoms m<sup>-3</sup>, (1.92±1.62)  $\times 10^5$  atoms m<sup>-3</sup>, and (4.17±1.37)  $\times 10^5$  atoms m<sup>-3</sup> in spring, summer, fall and winter, respectively. The level of  $^{129}\text{I}$  in winter was about two times higher than spring and fall, and 3.3 times higher than summer. Seasonal variation of  $^{129}\text{I}/^{127}\text{I}$  ratios was not such obvious as the concentrations of iodine isotopes. The mean  $^{129}\text{I}/^{127}\text{I}$  ratios were (119±185)  $\times 10^{-10}$  in fall and (124±112)  $\times 10^{-10}$ , slightly higher than those of (87.7±76.5)  $\times 10^{-10}$  in spring and (75.1±85.1)  $\times 10^{-10}$  in summer. Whereas, the ratios in all four seasons fell in the similar range as that of the whole year.

**Deleted:** 3

were the most months of 98.6 mm and 140 mm, respectively, accounting for 37% of the annual precipitation (Fig.2e) (Xi'an Bureau of Statistics, 2018). Taking the two months for exemplifying, sixteen aerosols were analysed with eight in rainy days and eight in non-rainy days.  $^{127}\text{I}$  and  $^{129}\text{I}$  concentrations fell in the ranges of  $1.88\text{--}4.93 \text{ ng m}^{-3}$  and  $(1.88\text{--}4.93) \times 10^5 \text{ atoms m}^{-3}$  in rainy days, respectively, were comparable to  $1.67\text{--}8.22 \text{ ng m}^{-3}$  and  $(0.44\text{--}7.25) \times 10^5 \text{ atoms m}^{-3}$  in non-rainy days. Although the concentration range was narrower in rainy days than non-rainy days, the data in same range suggest that precipitation does not significantly affect the variation of both iodine isotopes in aerosols. Furthermore, this conclusion is also supported by the fact that the frequent rainfall in October did not change iodine concentrations.▲

**Wind speed.** Wind speed affect not only the sources of iodine, but also the dispersion rate and retention in local atmospheric system. Controlled by topography, the annually prevailing wind direction is northeasterly wind in Xi'an and daily average wind speed was  $1.0\text{--}4.1 \text{ m s}^{-1}$  during the studied periods.  $^{127}\text{I}$  and  $^{129}\text{I}$  varied irregularly with changes of wind speed throughout the year (Fig.2f). These data indicated that small-scale atmospheric circulation limited within a local area unlikely had regular influence on variations of iodine isotopes, which is identical to the observation in Riso, Denmark (Zhang et al., 2016). Large-scale atmospheric circulation, however, might be profound, which will be discussed in the following section.

## Reference

Hou, X., Zhou, W., Chen, N., Zhang, L., Liu, Q., Luo, M., Fan, Y., Liang, W. and Fu, Y.: Determination of ultralow level  $^{129}\text{I}/^{127}\text{I}$  in natural samples by separation of microgram carrier free iodine and accelerator mass spectrometry detection, *Anal. Chem.*, 82(18), doi:10.1021/ac101558k, 2010.

Xi'an Bureau of Statistics: Xi'an Statistics Yearbook. [online] Available from: <http://tjj.xa.gov.cn/ptl/def/def/2017/zk/indexch.htm>, 2018.

Zhang, L., Hou, X. and Xu, S.: Speciation of  $^{127}\text{I}$  and  $^{129}\text{I}$  in atmospheric aerosols at Riso, Denmark: Insight into sources of iodine isotopes and their species transformations, *Atmos. Chem. Phys.*, 16, 1971–1985, 2016.

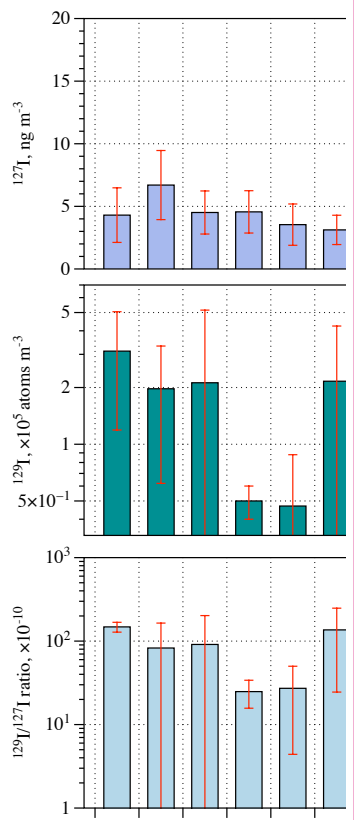
Zhang, L., Hou, X., Fu, Y., Fang, M. and Chen, N.: Determination of  $^{129}\text{I}$  in aerosols using pyrolysis and AgI–AgCl coprecipitation separation and accelerator mass spectrometry measurements, *J. Anal. At. Spectrom.*, 33, 1729–1736, doi:10.1039/C8JA00248G, 2018b.

130

**Formatted:** English (US)

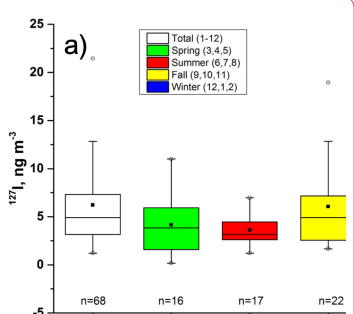
**Deleted:** SI-4. Quantitative characterization of the influence of EAM on variation of  $^{129}\text{I}$

To quantitatively characterize the influence of EAM on variation of  $^{129}\text{I}$ , z-normalized  $^{129}\text{I}$  concentrations and  $^{129}\text{I}/^{127}\text{I}$  ratios were used to build a quantitative model during winter monsoon and different stages of the summer monsoon including onset, active, break, revival and retreat (Fig.S8S).  $Z(^{129}\text{I})$  varies from -1.11 to 3.38 with a median value of -0.29, and  $z(^{129}\text{I}/^{127}\text{I}$  ratio) from -0.66 to 5.26 with a median value of -0.34. Based on the observation during 2017/2018 in the Guanzhong Basin, when  $z(^{129}\text{I})$  is less than -0.5 and  $z(^{129}\text{I}/^{127}\text{I}$  ratio) is smaller than 0, this period is in good agreement with the onset, active and revival stages of the EASM. During the stable active-stage, z-scores for  $^{129}\text{I}$  and  $^{129}\text{I}/^{127}\text{I}$  were minimal, which was followed by the second lowest value during the revival stage. The onset and break stage showed much larger fluctuation with z-scores changing from [-1]



**Deleted:**

... [2]



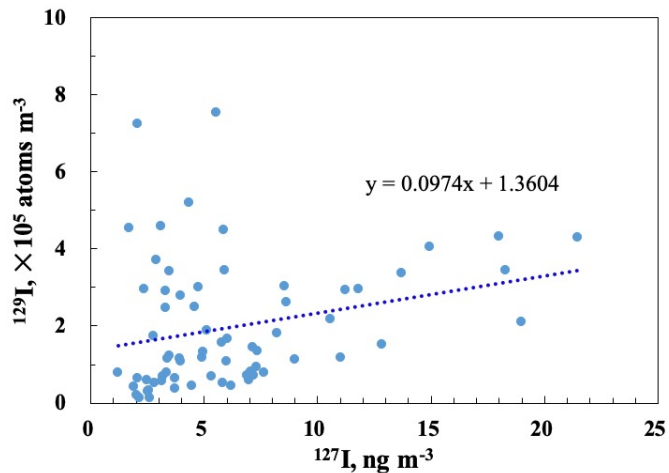
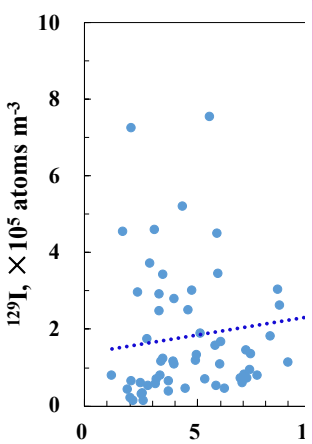


Fig. S1 Relationship between  $^{127}\text{I}$  and  $^{129}\text{I}$  with a weak correlation ( $R=0.33$ ,  $p<0.01$ ) between the two iodine isotopes. This indicates the two iodine isotopes have different sources and their temporal variation patterns were affected by different factors.

215



Deleted:

Deleted: S3

Deleted: , showing

Deleted: no

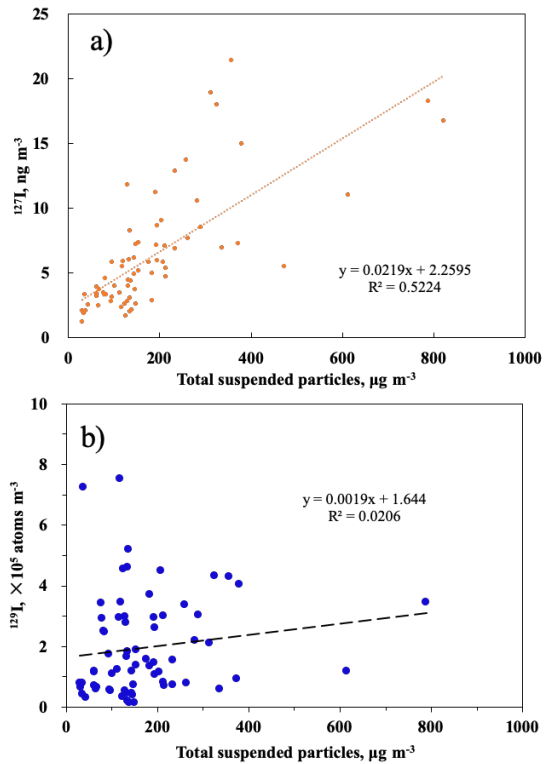
Deleted: 5

Formatted: Font: (Default) Times New Roman

Formatted: Not Highlight

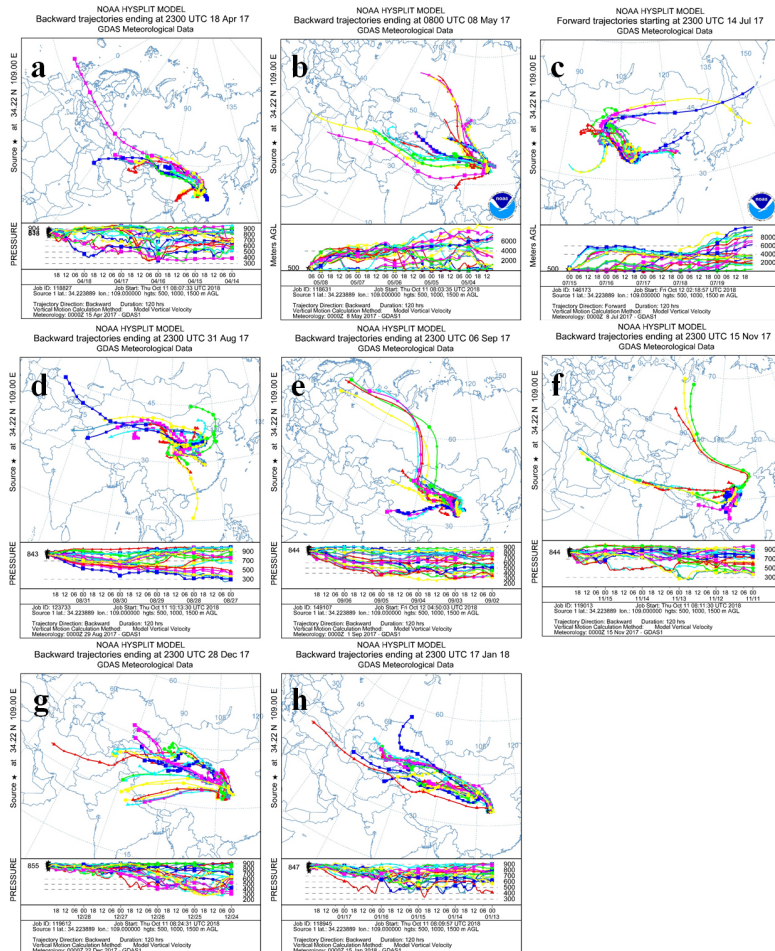
Deleted: significant

Deleted: 26



225 Fig. S2 Relationship between iodine isotopes and total suspended particles (TSP) in Xi'an, China (n=68), suggesting significant correlation between  $^{127}\text{I}$  and TSP, and no correlation between  $^{129}\text{I}$  and TSP. The results indicate  $^{127}\text{I}$  was sourced from local input and  $^{129}\text{I}$  was transported to the studied site externally.

Deleted: S4



|230 Fig. S3 Back trajectories analysis on date of a) 18th April, 2017; b) 18th May, 2017; c) 14th July, 2017; d) 31st August, 2017; e) 6th September, 2017; f) 15th November, 2017; g) 28th December, 2017; h) 17th January, 2018.

Deleted: S5

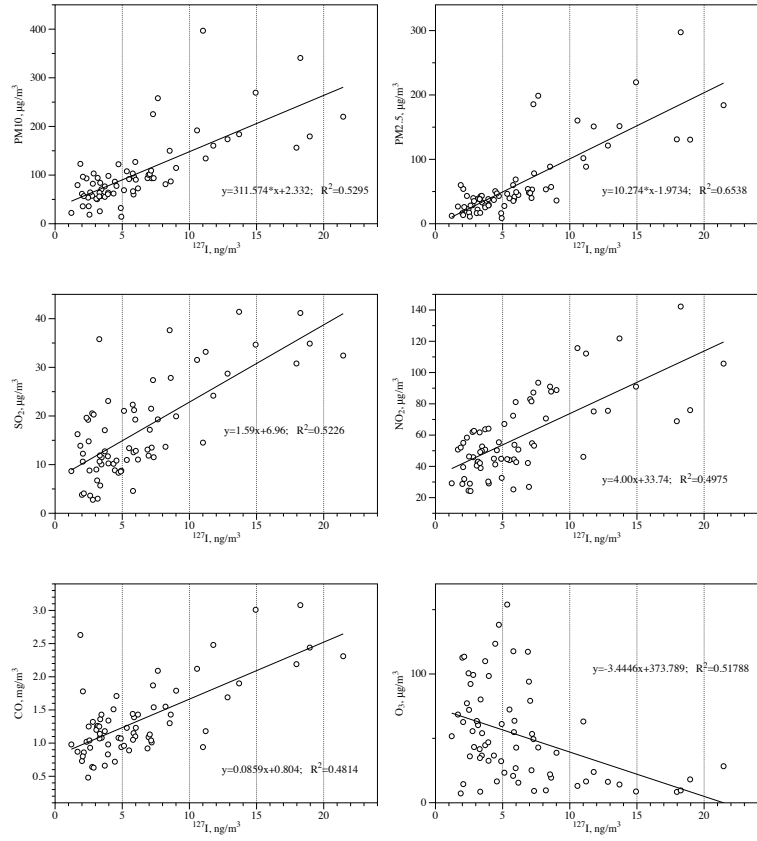
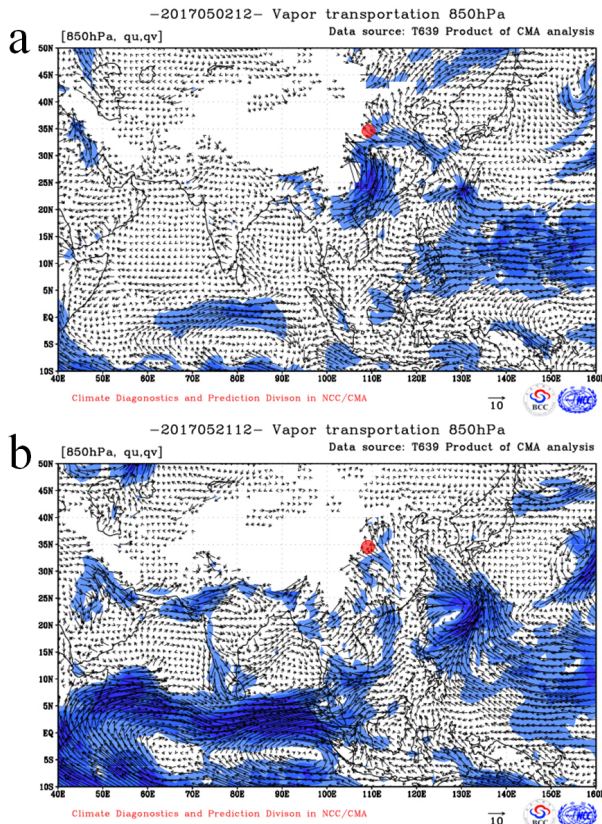


Fig. S4 Relations between  $^{127}\text{I}$  and air pollutants including PM10, PM2.5,  $\text{SO}_2$ ,  $\text{NO}_2$ , CO and  $\text{O}_3$ , showing significant correlation.

Deleted: S6



240

| Fig. S5 850 hPa water vapor transmission flow field on 2 May, 2017 (a), and 21 May, 2017 (b). Data from: <https://cmdp.ncc-cma.net/Monitoring/monsoon.php?ListElem=vt85>. The red dot in the figures is the sampling location, Xi'an, China.

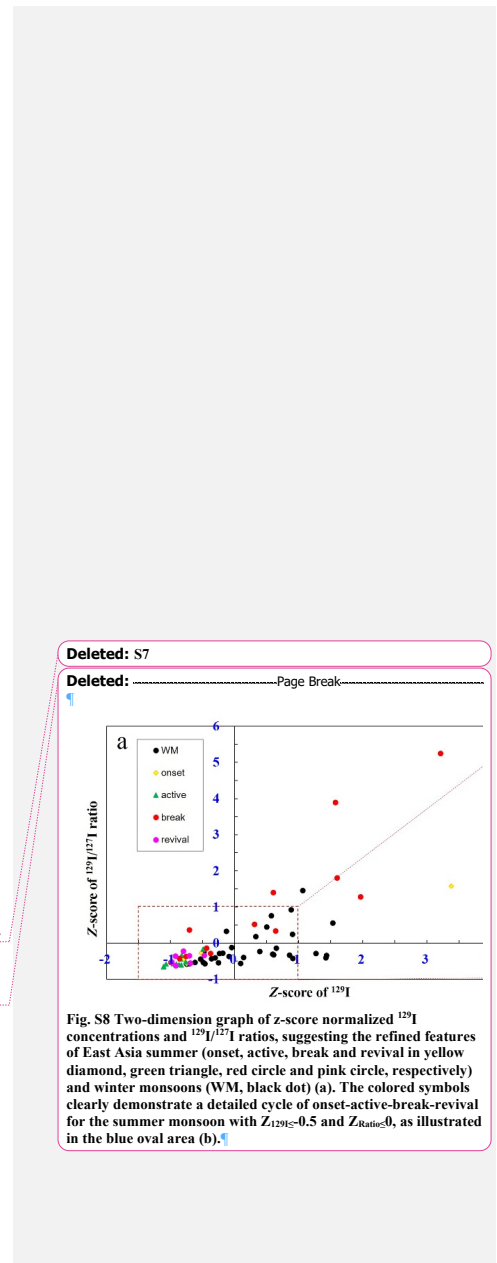


Table S1 Mean  $^{129}\text{I}$  concentrations and  $^{129}\text{I}/^{127}\text{I}$  ratios in three high-level periods (HLP) and two low-level periods (LLP)

No	Type	Start date	Stop date	$^{129}\text{I}$ , $\times 10^5$ atoms/m <sup>3</sup>		$^{129}\text{I}/^{127}\text{I}$ atomic ratio, $\times 10^{-10}$		Monsoon stage
				Average	RSD	Average	RSD	
1	HLP 1	28 Mar, 2017	22 May, 2017	2.37	91%	101 <sub>1</sub>	89%	WM and onset of SM
2	LLP 1	23 May, 2017	25 Jul, 2017	0.49	60%	28 <sub>5</sub>	65%	Active of SM
3	HLP 2	4 Aug, 2017	12 Sep, 2017	1.98	109%	155 <sub>1</sub>	141%	Break of SM
4	LLP 2	21 Sep, 2017	11 Oct, 2017	0.66	44%	40.1 <sub>1</sub>	44%	Revival of SM
5	HLP 3	13 Oct, 2017	20 Mar, 2018	2.41	44%	67 <sub>9</sub>	83%	SM retreat and WM advance then active

**Deleted:** Table S1 Iodine isotopes in aerosols from Xi'an, China from March 2017 to March 2018<sup>1</sup>

No

... [4]

**Deleted:** S2

**Formatted:** English (US)

**Deleted:** .30

**Deleted:** 47

**Deleted:** 45

**Deleted:** 5

**Deleted:** 87

<b>Page 3: [1] Deleted</b>	<b>Luyuan Zhang</b>	<b>12/14/19 4:14:00 PM</b>
<b>Page 3: [2] Deleted</b>	<b>Luyuan Zhang</b>	<b>12/12/19 6:13:00 PM</b>
<b>Page 3: [3] Deleted</b>	<b>Luyuan Zhang</b>	<b>12/12/19 6:13:00 PM</b>
<b>Page 9: [4] Deleted</b>	<b>Luyuan Zhang</b>	<b>12/12/19 6:01:00 PM</b>

## ***Response to Editor***

Dear Editor Dr. Jan Kaiser,

Thanks for your great effort on our manuscript.

According to the constructive comments from the two anonymous reviewers, we have carefully revised our manuscript, improved the language with the help of native English speaker and also corrected some writing errors.

Below are our major modifications in this manuscript.

1. Three figures (Figure 3, 4 and 6) have been moved from the Supplementary Information file to the manuscript to make our conclusions more convincing. The font of Figure 5 (original Figure 3) have been adjusted larger.
2. As commented by the reviewer, since iodine isotopes data did not distribute normally, in Table 1 we use Spearman correlation factors instead of Pearson correlation factors to indicate the relationship. Despite such a change, the correlation using Spearman shows almost same as Pearson, which does not affect our discussion and not change the final conclusions.
3. The statistical data, such as average values, standard deviations and correlation factors, have been carefully checked and recalculated. And we found a calculation mistake of average  $^{129}\text{I}/^{127}\text{I}$  atomic ratios, which should be  $(92.7 \pm 124) \times 10^{-10}$ , not  $(101 \pm 124) \times 10^{-10}$ . The reason for this mistake is that four data in spring 2018 were input into wrong columns. We apologize for our carelessness. All data have been corrected throughout the whole manuscript. The data correction did not change our conclusion.
4. The point of view about iodine's role on the formation of urban fine particles have been deleted. Although we found significantly positive correlation between iodine and air pollutants (except ozone), there still lack of direct evidence to prove that iodine contributes to the primary particle formation.

Best regards

Luyuan Zhang  
1/1/2020

## **Response to Interactive comment from Anonymous Referee #1**

The paper acp-2019-818-manuscript-version1 entitled “Temporal variation of  $^{129}\text{I}$  and  $^{127}\text{I}$  in aerosols from Xi'an, China: influence of East Asian monsoon and heavy haze events” provides interesting data for the distribution of iodine isotopes in the aerosols of part of China which are missing from the international data base. The paper has the potential for publication after revision as given below.

We are very grateful for the reviewer's positive and constructive suggestions and comments that make our manuscript better. According to the reviewer's comments, the main modifications are made in the revised version:

- 1) The language is further polished, including revising the grammar mistakes and shortening the long sentences;
- 2) The Figs 1, 3, S1, S2, S7 and S8 are reorganized and adjusted to make the discussion part more easily understood and convincing.

The comments are responded item by item as below.

1. The paper needs some linguistic revision as there are many grammatic mistakes.

**Response:** Sorry for such basic mistakes. We have checked throughout the context and revised all the linguistic mistakes.

2. Lines 44-45 “As a consequence of these point sources of  $^{129}\text{I}$ , the distribution of  $^{129}\text{I}$  is rather uneven (Snyder et al., 2010)? Where?

**Response:** These point sources of  $^{129}\text{I}$  have been listed in the reference of Snyder et al., 2010, including the principal nuclear reprocessing plants in Russia, UK, France, USA, Pakistan, China, Israel, India, South Africa and Argentina, nuclear accidents in Chernobyl, Former Soviet and Fukushima, Japan. For brief introduction, only references are cited here, not listing all these specific sources. This sentence has been revised to be “As a consequence of  $^{129}\text{I}$  releases from NFRPs, nuclear accidents and nuclear weapon testing sites, the global distribution of  $^{129}\text{I}$  is rather uneven (Snyder et al., 2010; Xu et al., 2015).”

3. The paragraph between lines 50 and 55 is long and difficult to follow and could be rewritten to focus on aims of the study.

**Response:** Line 50 has been separated into two parts, and revised to be “And those previous studies present the time series of  $^{129}\text{I}$  in aerosols in monthly resolution for the purpose of nuclear environmental monitoring. Such a low time-resolution is not sufficient to understand the source, transport and temporal variation pattern and its influencing factor of  $^{129}\text{I}$ .”

Line 51-55 paragraph has been reorganized into three sentences as below.

“Here, we present a day-resolution temporal variation of  $^{129}\text{I}$  and  $^{127}\text{I}$  in aerosols during 2017/2018 from a typical monsoonal zone, Xi'an city in the Guanzhong Basin of northwest of China, to make attempts to investigate the level, sources and temporal change characteristics of  $^{127}\text{I}$  and  $^{129}\text{I}$ . This study will help to establish a background value of  $^{129}\text{I}/^{127}\text{I}$  ratio serving the nuclear environmental safety monitoring. The possible influencing factors

on temporal variation of iodine isotopes are also explored, including meteorological parameters, East Asian monsoon (EAM) and heavy haze events.”

4. It is not clear how much time is the “a day-resolution” sampling reflects in term of iodine residence time in the atmosphere?

**Response:** Iodine residence time is closely related to its species and the associated states with particles, generally ranging from a few seconds to a few days for gaseous iodine species (Saiz-Lopez et al., 2012). For particle-associated iodine, its residence time is much dependent on particle size, varying from 0.1 day to 10 days (< 1 day for particles large than  $\sim 1 \mu\text{m}$ , and > 1 day for particles smaller than  $\sim 1 \mu\text{m}$ ) (Moyers and Duce, 1972). In this study, total suspended particles were sampled in a 24 h resolution, reflecting a relatively equilibrated state for gaseous-particle converted iodine and large particle-associated iodine with shorter residence time (< 1 day), and a more variable information of iodine in small particles. Such a time-resolution can benefit greatly our future work on speciation analysis of atmospheric iodine to dive deep into atmosphere iodine processes.

Referece:

Moyers, J.L., Duce, R.A., 1972. Gaseous and particulate bromine in the marine atmosphere. *J. Geophys. Res.* 77, 5330–5338. <https://doi.org/10.1029/jc077i027p05330>

Saiz-Lopez, A., Gómez Martín, J.C., Plane, J.M.C., Saunders, R.W., Baker, A.R., Von Glasow, R., Carpenter, L.J., McFiggans, G., 2012. Atmospheric chemistry of iodine. *Chem. Rev.* 112, 1773–1804.

5. Figures 1 a and b can be combined in one figure.

**Response:** Figure 1 has been reorganized. Figure 1b as an inset has been combined with 1a.

6. The results part needs further additions from the supplementary data including Figs. S1 and S2.

**Response:** The results including Figs. S1 and S2 in the supplementary data have been added into the manuscript.

7. Connection of iodine chemical forms ( $\text{I-127}$  and  $\text{I-129}$ ) from the sources and in the atmosphere may elucidate some of the inconclusive correlations and relationship to spatial and temporal atmospheric transport on short and long distances.

**Response:** We strongly agree with this comment. The short- and long-range transport of airborne iodine is strongly related with its chemical forms. The present study focuses on aerosol iodine, and the gaseous iodine ( $^{127}\text{I}$  and  $^{129}\text{I}$ ) sample collection and analysis are under way, while no data has been available at present. We do expect that further work on iodine chemical forms in air would give further understanding on the relationship.

8. More elaboration of weathering of basement rocks as a source of  $\text{I-129}$  will be interesting.

**Response:** In line 226-236, more explanation has been added as below. “Weathering of bed rock is not also a major source of airborne  $^{129}\text{I}$ , since weathering just contributes 5% of stable

iodine, and  $^{129}\text{I}$  in bed rock can be considered even lower the nature-produced  $^{129}\text{I}$  level because of the continuous decay.”

9. Addition of Figure S7 and S8 to the discussion section will enhance the understanding of the atmospheric transport pathways of the isotopes.

**Response:** For improving the understanding, Figure S8 and SI-4 discussion part have been moved to the manuscript. Considering too many figures and each importance, Figure S7 is still kept in the Supplementary Information.

10. More details on the paragraph in lines 100-104 can add clarity to general statement with respect to  $^{127}\text{I}$  distribution in China.

**Response:** Line 100-104 have been added more discussion of aerosol iodine in China. “Whereas, a similar range of TSP  $^{127}\text{I}$  was observed to be 4.5-22 ng m $^{-3}$  at coastal urban, Shanghai, China, and iodine concentration were lowest in summer and an increase occurred in fall and winter (Gao et al., 2010). Iodine associated with PM10 and PM2.5 were found to be 3.0-115 ng m $^{-3}$  and 4-18 ng m $^{-3}$ , respectively, in urban and island sites of Shanghai, slightly lower than TSP iodine (Cheng et al., 2017; Gao et al., 2010). The marine aerosol iodine offshore China was found below 8.6 ng m $^{-3}$  during the XueLong cruise from July to September 2008 (Xu et al., 2010). These results suggest a relatively high aerosol  $^{127}\text{I}$  level in both inland and coastal urbans in China.”

Referece:

Cheng, N., Duan, L., Xiu, G., Zhao, M., Qian, G., 2017. Comparison of atmospheric PM2.5-bounded mercury species and their correlation with bromine and iodine at coastal urban and island sites in the eastern China. *Atmos. Res.* 183, 17–25.  
<https://doi.org/10.1016/j.atmosres.2016.08.009>

Gao, Y., Sun, M., Wu, X., Liu, Y., Guo, Y., Wu, J., 2010. Concentration characteristics of bromine and iodine in aerosols in Shanghai, China. *Atmos. Environ.* 44, 4298–4302.  
<https://doi.org/10.1016/j.atmosenv.2010.05.047>

Xu, S., Xie, Z., Li, B., Liu, W., Sun, L., Kang, H., Yang, H., Zhang, P., 2010. Iodine speciation in marine aerosols along a 15000-km round-trip cruise path from Shanghai, China, to the Arctic Ocean. *Environ. Chem.* 7, 406–412.

11. The anthropogenic source for I-127 is mainly related to coal consumption (local source) whereas the I-129 source is mainly related to far away transport. It will be good to provide some details of how these isotopes are associated in the atmosphere with respect to airmasses altitude, chemistry and residence time of the isotope.

**Response:** The mechanism for iodine association with particles with many uncertainties, generally has two pathways, iodine compounds as primary nuclei during fine particle formation, and adsorption onto naturally occurring particles (Garland, 1967; Saiz-Lopez et al., 2012). In section 4.2.2, association of  $^{127}\text{I}$  and  $^{129}\text{I}$  with particles has been elucidated in respect of nucleation process and residence time. However, some interpretations need more evidence. Chemical processes could definitely affect iodine species in aerosols, such as

inorganic iodide and iodate, the former of which has been found in a large proportion of inorganic iodine likely because of the presence of reductant  $\text{SO}_3$  (Zhang et al., 2016). As this paper focuses on the temporal variation of total iodine isotopes and there is no more data to suggest that chemical process would significantly affect the total iodine change, therefore, it is hard to discuss the influence of chemical processes on iodine bound to particles. Our future work on aerosol iodine species will put more efforts on this point. In section 4.2.3, “Furthermore, the back trajectory analysis also showed that the low  $^{129}\text{I}$  level on April 18 can be partially attributed to an  $^{129}\text{I}$ -poor low-altitude air mass (< 900m) (Fig.S3a), since either they might be formed in  $^{129}\text{I}$ -poor inland areas, not from the  $^{129}\text{I}$ -rich European area, or long-range transported  $^{129}\text{I}$  in low-altitude air mass could be easily lost by the topographic countercheck (Dong et al., 2018).” has been modified to explain the influence of airmass altitude.

Referece:

Dong, Z., Shao, Y., Qin, D., Zhang, L., Hou, X., Wei, T., Kang, S., Qin, X., 2018. Insight Into Radio-Isotope  $^{129}\text{I}$  Deposition in Fresh Snow at a Remote Glacier Basin of Northeast Tibetan Plateau, China. *Geophys. Res. Lett.* 0. <https://doi.org/10.1029/2018GL078480>

Garland, J.A., 1967. The adsorption of iodine by atmospheric particles. *J. Nucl. Energy* 21, 687–700.

Zhang, L., Hou, X., Xu, S., 2016. Speciation of  $^{127}\text{I}$  and  $^{129}\text{I}$  in atmospheric aerosols at Risø, Denmark: Insight into sources of iodine isotopes and their species transformations. *Atmos. Chem. Phys.* 16, 1971–1985.

12. May be good to make the text in Figure 3 in larger font.

**Response:** The font in Figure 3 has been adjusted larger.

13. Although the authors pointed out the possible use of air masses transport to predict iodine sources and impact on future iodine distribution, it is still not clear how the iodine data enhance our understanding of the climate or atmospheric circulation.

**Response:** Here we use a set of day-resolution iodine isotopes data to establish the crucial linkage with East Asia monsoon system and meteorological conditions. On this basis, long-term observation of iodine isotopes would refresh the understanding of climate change, not just one-year short-term iodine data presented in this paper. Moreover, high time-resolution iodine data in combination with modelling should be expected. Before make the application on climate and atmospheric circulation, plenty of questions have to be well answered, for instance, how airborne iodine species like and interact with each other.

## ***Response to Interactive comment from Anonymous Referee #2***

This manuscript reports the concentrations and ratios of  $^{129}\text{I}$  and  $^{127}\text{I}$  in aerosol samples collected over a period of approximately one year at Xi'an in China. The data are interpreted in terms of the dominant sources and transport pathways of these iso-topes to the site, and the discussion considers the influence of the fluctuating modes of the East Asian Monsoon on the observed record. The subject matter is highly relevant for Atmospheric Chemistry and Physics and the authors have a track record of producing high quality data from the demanding measurements employed. However, the manuscript suffers from a number of shortcomings, including factual errors and subjective and unsupported interpretations. I think that this will be an excellent contribution once these have been addressed. There are many minor errors in the English used, but the meaning of the manuscript is still clear.

We thank the admirable reviewer for the positive evaluation and providing us these constructive comments. The reviewer has a very deep understanding and rich experience on iodine study area. It is also our honor to have such valuable suggestions and comments, which significantly improve the quality of this manuscript. We are in complete agreement that some interpretations are not fully supported by the current evidence, for instance, the associated mechanisms of locally released  $^{127}\text{I}$  and externally input  $^{129}\text{I}$  with particles in urban atmosphere, whether they are mainly involved into primary particle formation or scavenged by existing particles. To answer this, more research is needed in the future.

Following the detailed comments, we have carefully checked throughout the content, made all English corrections and revised the manuscript. Below are our responses the comments item by item.

### **Major comments**

1. There are numerous instances of inconsistent units being used for iodine concentrations for the Xi'an site in the Results section (line 77 onwards). In the text, the units are frequently given as micrograms per cubic metre, while in the figures and supplementary material the units are nanograms per cubic metre. Since the numbers in both cases are the same, one of the units must be incorrect. I assume that the units should actually be nanograms per cubic metre, but please check and correct.

**Response:** Sorry for the basic mistakes on the incorrect unit of  $^{127}\text{I}$  concentrations. As the reviewer commented,  $^{127}\text{I}$  concentrations in aerosols should be nanograms per cubic metre, not microgram per cubic metre. All the unit mistakes have been carefully checked and revised.

2. On line 91 the authors state that "A weak correlation between  $^{129}\text{I}$  and  $^{127}\text{I}$  was found with a Pearson correlation coefficient of 0.34 ( $p=0.01$ ) for the whole year data, while no significant correlation between the two iodine isotopes in each season at the level of 0.05 (Table 1 and Fig. S3)." This does not agree with the statement made in the caption to Fig S3: "Relationship between  $^{127}\text{I}$  and  $^{129}\text{I}$ , showing no significant correlation ( $R=0.265$ ) between the two iodine isotopes". Why do these statements not agree? Since it is apparent from Fig S3 that the dataset is not normally distributed, I would suggest the authors use a non-parametric regression method (such as Spearman's Rank Correlation) instead of Pearson's for

all regression analysis in the manuscript. This will give far more robust results. Perhaps Figure S3 might be more informative if plotted with different symbols for the time periods of interest.

**Response:** According to the reviewer's comment, we use Spearman coefficient to discuss the correlation. Although  $^{127}\text{I}$  and  $^{129}\text{I}$  data are not normally distributed, Pearson and Spearman coefficients are typically identical. The inconsistency between Table 1 and Figure 3 is resulted from numbers of data used for calculation. The Pearson coefficient of 0.26 is used for all the 68 data points.

It is a good idea to replot Figure S3 using different symbols. We have tried in this way as shown below. The Figure 1 below is plotted with different symbols and fitting trends for the four seasons, clearly showing the concentration distribution in different seasons. While no more information could be obtained because the previous Figure S1 and S2 (now move to the context as Figure 3 and 4, respectively) have clearly showed the information. Therefore, Figure S3 is kept as before only with a small revision by changing the Pearson correlation coefficient to Spearman coefficient.

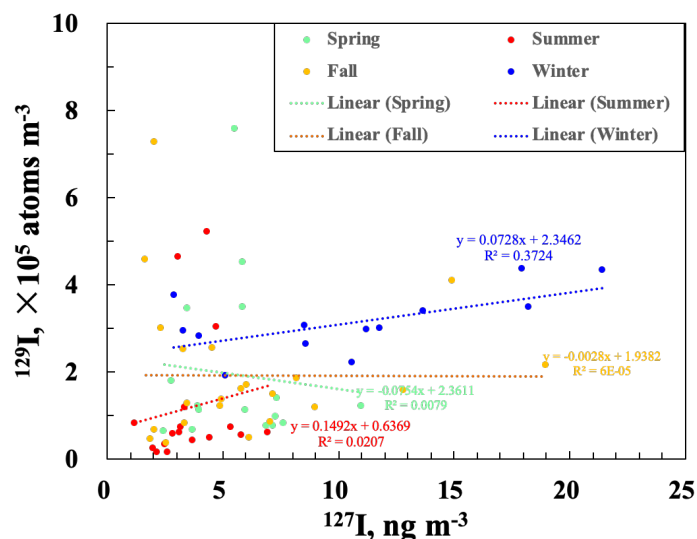


Figure 1. Relation of  $^{127}\text{I}$  and  $^{129}\text{I}$  indicated by different symbols and trend lines for four seasons

3. I am not quite sure how the authors have used the values published in Saiz-Lopez et al., 2012 to compare to the results obtained at Xi'an. In Table 5 of Saiz-Lopez, aerosol iodine concentrations of up to 25 ng m<sup>-3</sup> and >3.3 ng m<sup>-3</sup> are quoted for open ocean and continental sites respectively. These do not seem to relate to the values for "terrestrial" (1 ng m<sup>-3</sup>) and "marine" (<10 ng m<sup>-3</sup>) air quoted in lines 100 & 101. The higher values in Saiz-Lopez et al. also do not give strong support to the statement in the last sentence of this paragraph (lines 102-103).

**Response:** We agree with the reviewer that this statement and citation of Saiz-Lopez is vague. Therefore, we revise lines 100-104, and also add more data in China. This paragraph was modified as below.

"The level of  $^{127}\text{I}$  concentrations, in particular in winter, is much higher than those in continental sites (below 0.61 ng m<sup>-3</sup> in South Pole and 2.7-3.3 ng m<sup>-3</sup> in the Eastern

Transvaal), and comparable to those in coastal and ocean sites (typically below 20 ng m<sup>-3</sup>, and up to 24 ng m<sup>-3</sup> in tropic marine aerosols) (Saiz-Lopez et al., 2012). A similar range of TSP <sup>127</sup>I was observed to be 4.5-22 ng m<sup>-3</sup> at coastal urban, Shanghai, China, showing lowest in summer and an increase occurred in fall and winter (Gao et al., 2010). Iodine associated with PM10 and PM2.5 were found to be 3.0-115 ng m<sup>-3</sup> and 4-18 ng m<sup>-3</sup>, respectively, in urban and island sites of Shanghai, slightly lower than TSP iodine (Cheng et al., 2017; Gao et al., 2010). The maximum of marine aerosol iodine offshore China was found below 8.6 ng m<sup>-3</sup> during the XueLong cruise from July to September 2008 (Xu et al., 2010). These results suggest a relatively high aerosol <sup>127</sup>I level in both inland and coastal urbans in China.”

4. The statement about natural sources of iodine (lines 104-105) comes from a rather old source (Fuge & Johnson, 1986). While it is true that sea spray contributes iodine to the atmosphere, we now know that gas-phase emissions of iodine from the ocean are a much stronger source (see, for example, Carpenter et al., 2013 – which the authors cite later in the manuscript). Thus the study of He (2012) which apparently used sodium concentrations to estimate the seaspray contribution of iodine to precipitation at Zhouzhi county almost certainly greatly underestimated the “direct contribution of ocean”. (The citation of He 2012 in the reference list does not give sufficient information for the source to be found).

**Response:** Accept. The reference “Carpenter et al., 2013” is added as “Natural iodine is from marine emission through sea spray, weathering of base rock and continental release through vegetation and suspended soil particles (Carpenter et al., 2013; Fuge and Johnson, 1986).”

Because of direct emission of gaseous iodine from sea surface, we agree that marine iodine contribution in the reference of He (2012) would be underestimated when using Na<sup>+</sup> as reference element for calculation. In this reference, spatial distribution of iodine in rainwater and surface freshwater were also reported. Despite being underestimated, sea source contribution of iodine showed a decline trend with increasing distance from the sea until 100 km, over which no significant change of marine contribution could be found. Our study site, Xi'an, is an inland city about 900 km from the nearest sea. It is therefore not likely that marine source (including sea spray, direct volatilization and gaseous emission) is the major contribution of iodine.

5. In lines 114 - 118, the authors attempt to balance estimated emissions of iodine from terrestrial soil and vegetation (from Sive et al., 2007) against an estimate of iodine deposition flux. There is insufficient detail given of how this deposition flux calculation was done, but it appears to be based on “dust fall”. Better explanation is required if this calculation is to be understood. Does “dust” here refer to mineral dust? If so, why should its deposition be specifically associated with the deposition of iodine? How exactly was the calculation done? The value given for the terrestrial emission flux (2.27 ug m<sup>-2</sup> d<sup>-1</sup>) does not seem to agree with the value given by Sive et al. (2.7 ug m<sup>-2</sup> d<sup>-1</sup>). How reliable is the comparison likely to be when the emission flux estimate is derived entirely from observations in North America, where vegetation types and land surfaces are different from the study region here?

**Response:** As commented by the reviewer, the dry deposition flux of <sup>127</sup>I is not specific enough. In this manuscript, the dry deposition flux of <sup>127</sup>I is calculated by <sup>127</sup>I mass concentration in total suspension particles multiplying the average dust fall flux. Since it is hard to know the deposition velocity of total suspension particles, we use dustfall flux for approximate calculation. Dust in this manuscript refer to natural dust, not but including mineral dust in air.

The dustfall is collected by wet method, i.e. a 20 cm in diameter  $\times$  30 cm height container with enough deionized water. There are 14 sampling sites in Xi'an. The natural dustfall ranges within 4.5-47.8 t (km $^{-1}$  30 d $^{-1}$ ) with an annual mean of 13.2 t (km $^{-1}$  30 d $^{-1}$ ). According to the reference Yang et al., 2017 listed below, the annual dustfall flux in 2014 at Qujiang District, about 2km from our sampling site was  $11.76 \pm 3.65$  t (km $^{-1}$  30 d $^{-1}$ ). The uncertainty for the dustfall flux is 31%, and iodine concentration uncertainty is within 5%, resulting in a total uncertainty of 32%. We have given a more detailed description about this calculation in the context.

Reference: Yang Wenjuan, Chen Ying, Zhao Jianqiang, et al. Spatial and temporal variation of atmospheric deposition pollution in Xi'an City. Environmental Science & Technology (in Chinese), 2017, 40(3):10-14.

In reference Sive et al., 2007, 2.7  $\mu\text{g m}^{-2} \text{d}^{-1}$  and 2.27  $\mu\text{g m}^{-2} \text{d}^{-1}$  were presented in abstract and Section 5, respectively. The value of 2.7  $\mu\text{g m}^{-2} \text{d}^{-1}$  just occurred in Abstract, lacking of calculation details. The average terrestrial emission flux (2.27  $\mu\text{g m}^{-2} \text{d}^{-1}$ ) was estimated, on a global basis, over an active season of 240 days, together with biome areas for temperate forest and wood lands ( $28.5 \times 10^{12} \text{ m}^2$ ) and temperate grasslands ( $31.9 \times 10^{12} \text{ m}^2$ ). Therefore, we cite the value of 2.27  $\mu\text{g m}^{-2} \text{d}^{-1}$  because of its clear mathematical description.

The terrestrial emission flux by Sive et al., 2007 should be much higher than that in urban environment, since a part of the urban land is covered by houses and roads without iodine emission.

6. Have the authors considered the influence of seasonal changes in boundary layer height on aerosol iodine concentrations? These could potentially be significant, and could cause changes in surface level concentrations even when emission fluxes are constant.

**Response:** This is a very good point to consider the boundary layer height, which is closely related with air pollution, and can indicate the vertical dispersion scale of air pollutants by thermal turbulent mixing. Not only the boundary layer height (BLH), but also the atmospheric stability (AS) could directly affect the concentration and time-space distribution of pollutants. And they might be important factors to control the variation of iodine isotopes. To be honest, at present, we have no idea about the impact. In future, we would like to make further investigation for 3-4 years to evaluate, to what extent the BLH and AS have influence on variation of iodine isotopes.

7. While I understand that the authors' estimate of the potential contribution of coal combustion to aerosol iodine loading at their study site is only intended as a first-order estimate, I do not think that they have sufficient information to attempt it. The assumption that surface iodine emissions are mixed through the entire troposphere (i.e. to 10 km) is certainly not realistic, since only a small proportion of emissions are likely to leave the boundary layer ( $\sim 1$  km). This implies an order of magnitude greater iodine concentration derived from coal, which does not appear to be plausible.

**Response:** We agree that this calculation of aerosol iodine from coal iodine is not plausible, so the following statement has been deleted. "The area of the Guanzhong Basin is  $3.6 \times 10^4 \text{ m}^2$ , and the height of troposphere is taking as 10 km. Then,  $^{127}\text{I}$  concentration in the air is about 250  $\text{ng m}^{-3}$ . The particle-associated iodine accounts for approximately 10%-20% (Hasegawa

et al., 2017). Thus,  $^{127}\text{I}$  in aerosols can be estimated to be about  $25\text{-}50\text{ ng m}^{-3}$ . The estimated value is comparable with the  $^{127}\text{I}$  peak values in winter, but about ten times higher than the less polluted aerosol  $^{127}\text{I}$  concentrations ( $1.21\text{-}9.01\text{ ng m}^{-3}$ )."

8. Lines 221 – 222: "Two severe dust storm events occurred in Xi'an in 17-18 April and 4-6 May, 2017, as shown by the peaks of air quality index (AQI) of 268 and 306, respectively (Fig. 2e)." There is only one peak in AQI visible in Fig 2e in this time period. Please explain or amend.

**Response:** Thanks for pointing out this flaw. It is right that only the first dust storm in 17-18 April have been shown in Figure 2e, because no sample was analysed during the second sand storm in 4-6 May. Thus, we give the AQI values for the two events. Below is Figure 2 for the daily measurement of AQI, from which we can see two peaks of the dust storm events. After careful thinking and for simplification, we decide to use AQI data on the days with iodine isotopes values. Thus, we have revised the statement as "Two severe dust storm events occurred in Xi'an in 17-18 April and 4-6 May, 2017, as indicated by the peaks of air quality index (AQI) of 268 and 306, respectively."

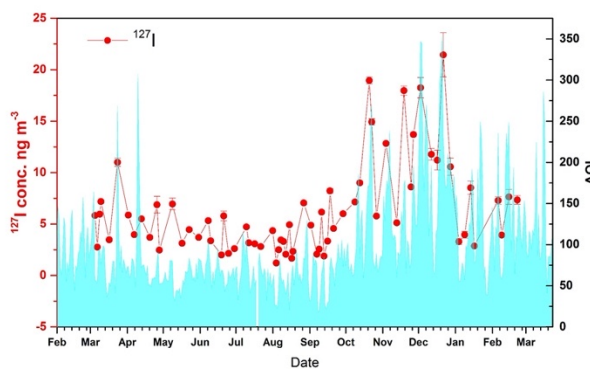


Figure 2. Temporal variation of  $^{127}\text{I}$  and AQI during March 2017 to March 2018, showing the correlation of  $^{127}\text{I}$  and AQI.

9. Please give further explanation of the significance of the "low-altitude air mass" mentioned on line 232.

**Response:** Further explanation has been added as below. "Furthermore, the back trajectory analysis also showed that the low  $^{129}\text{I}$  level on April 18 can be partially attributed to an  $^{129}\text{I}$ -poor low-altitude air mass (< 900m) (Fig.S3a). This is because either the low-altitude air mass might be formed in  $^{129}\text{I}$ -poor inland areas, not from the  $^{129}\text{I}$ -rich European area, or long-range transported  $^{129}\text{I}$  in low-altitude air mass could be easily lost by the topographic countercheck (Dong et al., 2018)."

10. On lines 250 – 254 (and later in the manuscript) the authors discuss the possibility that the aerosol iodine they observed might have formed through primary nucleation. While there are relationships between iodine concentration and those of other species associated with nucleation (e.g. SO<sub>2</sub>, Fig S6), it is also apparent that the concentration of SO<sub>2</sub> is three orders of magnitude greater than that of aerosol iodine. There is no evidence available in this dataset that would make it possible to determine whether iodine is incorporated into aerosol in Xi'an via primary formation or secondary uptake onto existing particles. I therefore suggest that

discussion of the iodine aerosol formation mechanism can only be speculation, and it would be better to remove it entirely.

**Response:** We agree that the mechanism of iodine association with particle is not well understood on the basis of our data. Therefore, these corresponding statements in Section 4.2.2 has been removed as below.

“Typically, new particle formation occurs in two distinct stages, i.e., nucleation to form a critical nucleus and subsequent growth of the freshly nucleated particle to a larger size (Zhang et al., 2015). It is widely accepted that iodine is involved into the formation of fine particles, and increasing investigations have been carried out in coastal and open sea areas (Saiz-Lopez et al., 2012). However, in megacities with severe air pollution, the role of iodine on formation and development of heavy haze events is far not understood. Iodine-mediated particles were suggested to be formed from highly concentrated, localized pockets of iodine oxides as primary nucleation, and to rapidly grow by uptake of  $\text{H}_2\text{SO}_4$ ,  $\text{H}_2\text{O}$ ,  $\text{NO}_2$ , short chain dicarboxylic acids, gaseous iodine and other gaseous species (Saiz-Lopez et al., 2012). Winter urban air in Xi'an provides two requirements of sufficiently high iodine concentrations and the presence of high levels of aerosol nucleation precursors, such as  $\text{SO}_2$ ,  $\text{NH}_3$ , amines, and anthropogenic VOCs.”

“In spring and summer, iodine is probably associated with primary matters and secondary organic aerosols due to low level of air iodine and greatly increased artificial and biogenic VOCs (Feng et al., 2016). In fall and winter when the key aerosol nucleation precursors are noticeably elevated, the significantly positive correlation between  $^{127}\text{I}$  and these precursors indicates that locally emitted iodine is likely involved into formation of secondary inorganic aerosols, while externally input  $^{129}\text{I}$  may not occur in the nucleation of secondary inorganic aerosols.”

“The minimum in ozone concentrations on 15 November and 14 December, 2017 may support iodine-containing aerosol nucleation process, in which ozone acted as oxidant and reactant to form iodine oxidizes, and aggregated into high valence iodine oxidizes (Saiz-Lopez et al., 2012). This study suggests iodine is closely related to aerosol formations, and high level of iodine likely facilitates the growth of fine particles along with major aerosol precursors particularly during haze episodes.”

11. In section 4.2.3 the authors make a convincing case for the influence of interactions with the East Asian Monsoon on long-range  $^{129}\text{I}$  transport to the study site. I am not familiar with the EAWM index mentioned on line 303, but I wonder whether it is possible to make more use of this when exploring the variations in iodine isotope concentrations and their ratios during the study. Can it be plotted on Fig 2? The “z-score” approach discussed on lines 333 – 336 would be more convincing if it could be combined with some quantitative indicator of EAM strength.

**Response:** When we prepare this manuscript, we have actually plotted the EAWM and EASM indexes with  $^{129}\text{I}$  variation as shown by Figure 3 below. It is quite interesting that the fluctuation of  $^{129}\text{I}$  concentrations have some close relation with these indexes. Whereas, this is our first try to link the monsoon strength with  $^{129}\text{I}$  variation, so that we could not understand it deeper at present. We also expect to do further work on this.

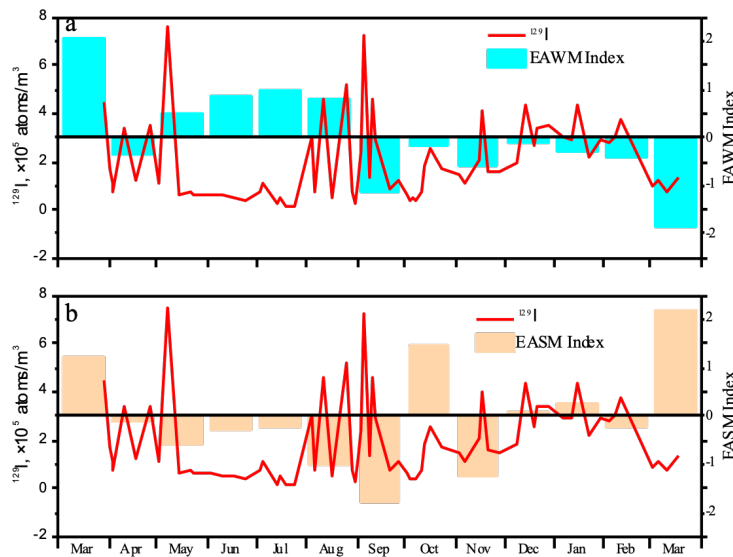


Figure 3. Variation of  $^{129}\text{I}$  and EAWM (top) and EASM (bottom) indexes during 2017-2018

The “z-score” method gives clear indications for different monsoon stages, so Figure S8 has been moved into the manuscript as Figure 6, together with the statements.

12. On lines 301 – 302 it is stated that “In addition, the  $^{129}\text{I}$  level in March 2018 was much less than that in March 2017”. This is certainly true, and in fact the  $^{129}\text{I}$  concentration in March 2018 is very similar to that in the two LLP periods. Why did the authors choose to include these samples in the HLP period?

**Response:** We can find that the fluctuation of  $^{129}\text{I}$  is very large during the HLP periods, but with low concentrations down to the level same as LLP periods. In March 2018, only four data are available. Considering this period is under control of EAWM, these low values were likely as a consequence of fluctuation, and therefore categorized into the HLP period.

13. The statement on line 338 that the iodine isotope ratio shows “relatively weak fluctuation” seems rather subjective, and quite surprising given the relative standard deviation quoted for the parameter of  $>120\%$ . There are strong variations in the ratio during the HLP 2 period, which do not appear to be consistent with the statement on line 339 about background levels.

**Response:** Agree. The subjective statement “Both two iodine isotopes show apparently temporal changes in northwestern China, while  $^{129}\text{I}/^{127}\text{I}$  ratios show relatively weak fluctuation (Fig.2c).” has been deleted.

14. Minor comments Line 61: replace “combing” with “combined”? Line 75: replace “ration” with “ratio” Line 178-179: Toyama et al. is cited both at the beginning and end of this sentence, but with different years. Please correct. Line 211: I think the correct units for ozone concentration here should be ppbv, not pptv.

**Response:** Line 61, “combing” has been revised to be “combined”;  
 Line 75, “ration” has been revised to be “ratios”;

Line 178-179: "Toyama et al. (2012)" at the beginning of this sentence has been revised to "Toyama et al. (2013)", and the citation at the end of the sentence has been deleted.

Line 211: We appreciate the reviewer for this unit mistake. After carefully checking the cited reference, ozone concentration here has been revised to be ppbv.